

MODELLING AND OPTIMIZATION OF A SG TYPE SEISMOMETER
PROPORTIONAL TO THE ELONGATION

by

Mehmet Çakan

B.S. , Electrical and Electronics Engineering, Boğaziçi University, 2009

Submitted to the Institute for Graduate Studies in
Science and Engineering in partial fulfillment of
the requirements for the degree of
Master of Science

Graduate Program in Electrical and Electronics Engineering
Boğaziçi University

2012

ACKNOWLEDGEMENTS

The author would like to express his sincere gratitude to Prof. Okay Kaynak for the opportunity to work with him for this thesis. Without his guidance, help, encouraging trust and support this work would not be possible.

He would also like to express his sincere gratitude to his beautiful wife Zübeyde Çakan for her endless patience and support while he spent days and nights for this work.

ABSTRACT

MODELLING AND OPTIMIZATION OF A SG TYPE SEISMOMETER PROPORTIONAL TO THE ELONGATION

In this thesis, a new SG type seismometer is modelled and its counterforce constant is optimized to have an increased period length large enough to make seismic measurements. In the first part of the thesis a “Kinematic Model of the Seismometer” is built in simulink. It consists of three subsequent submodels which are an “Idealized Pendulum Angle Model”, a “Magnetic Counterforce Effect on Period Model” and a “Drag Force Model”. The problem of period increase with magnetic counterforce is defined in the second part of the thesis. The simulink models, which are built in the first part, are used to study and to solve this optimization problem. The binary search is used to find the best magnetic counterforce constant value and the golden section search is used to find the highest possible period value which grants harmonic oscillation and lowest error output. As a result; a magnetic counterforce constant value is reached for every desired period length, which is possible to reach due to the mechanical restrictions of the pendulum. It is proven that with an optimized magnetic counterforce constant, a SG type seismometer will have an increased period value, which grants the seismometer to become as effective as a high cost seismometer.

ÖZET

SALINIMLA DOĞRU ORANTILI ÇALIŞAN SG TİPİNDE BİR SİSMOMETRENİN MODELLENMESİ VE OPTİMİZASYONU

Bu tezde SG tipinde çalışan yeni bir sismometre modellenmiş ve onun karşı kuvvet sabiti tutarlı sismik ölçümler yapmasına yeterli olacak seviyeye optimize edilmiştir. Tezin ilk kısmında “Sismometrenin Kinematik Modeli” Simulink’te üç alt model kurulup bu modellerin uygun bir şekilde birleştirilmesiyle oluşturulmuştur. Bu modeller sırasıyla “Basit Sarkaç Açılı Modeli”, “Manyetik Karşı Kuvvet’in Periyoda Etki Modeli” ve “Havanın Sürtünme Kuvveti Modeli”dir. İkinci kısımda ilk olarak karşı kuvvet sabitiyle periyot arttırma problemi tanımlanmıştır. Ayrıca ilk kısımda oluşturulan Simulink modelleri yardımıyla bu optimizasyon problemi için bir çözüm yoluna ulaşılmıştır. Sismometrenin kendi özgün değerlerine bağlı olarak çalışabileceği en ideal periyot değerine Golden Section Search metoduyla yaklaşmıştır. Bu sırada istenilen periyot değerini sağlayacak manyetik karşı kuvvet sabitine de Binary Search metoduyla yaklaşmıştır. Sonuç olarak sismometrenin fiziksel sınırları içerisinde bulunan periyot değerlerine ulaşmasını sağlayan manyetik karşı kuvvet sabit değeri bulunabilmektedir. Bu sayede bu tezde optimize edilmiş bir karşı kuvvet sabitiyle SG tipinde çalışan bu yeni sismometrenin periyot seviyesinin yükseltilerek, yüksek maliyetli ve yüksek hassasiyetli sismometreler seviyesinde ölçüm yapmaya yetecek bir seviyeye çıkarılabileceği gösterilmiştir.

TABLE OF CONTENTS

ACKNOWLEDGEMENTS	iii
ABSTRACT	iv
ÖZET	v
LIST OF FIGURES	viii
LIST OF SYMBOLS	xi
LIST OF ACRONYMS/ABBREVIATIONS	xii
1. INTRODUCTION	12
1.1. Seismic Waves	12
1.1.1. Body Waves	12
1.1.2. Surface Waves	13
1.2. Detection and Measurement Methods	14
1.2.1. Houfeng Didong Yi	14
1.2.2. C-Spring Seismometer	15
1.2.3. Teleseismometer	15
1.2.4. Lehman Seismometer	16
1.2.5. Shackleford Gundersen Seismometer	17
1.3. Former Work and Past Experience	17
2. MATHEMATICAL AND SIMULINK MODELLING	19
2.1. Mathematical Model of an SG Type Seismometer	19
2.1.1. Mathematical Model of the Simple Pendulum (Force Derivation) ..	24
2.1.2. Simulink Model of the Simple Pendulum	25
2.1.3. Mathematical Model of Magnetic Counterforce	26
2.1.4. Simulink Model of Magnetic Counterforce	30
2.1.5. Mathematical Model of Air Drag Force	31

2.1.6.	Simulink Model of Air Drag Force	32
2.1.7.	Simulink Model of the Real Pendulum with Magnetic Counterforce	33
2.2.	Other Required Models	34
2.2.1.	Signal Generator 1	34
2.2.2.	Signal Generator 2	37
2.2.3.	Transmitter Receiver model	37
3.	OPTIMIZATION	39
3.1.	Theoretical Background	39
3.1.1.	Binary search method	40
3.1.2.	Golden section search method	40
3.2.	Problem Definition	41
3.3.	Solution Approach	42
3.3.1.	Magnetic Counterforce Optimization	42
3.3.2.	Oscillation Period Optimization	46
4.	CONCLUSION	52
4.1.	Summary of Achievements and Conclusion	52
4.2.	Future Work	53
	APPENDIX A: PENDULUM PERIOD CORRECTION	55
	APPENDIX B: OTHER SEISMOMETER BLOCK FIGURES	58
	APPENDIX C: MATLAB ALGORITHMS AND FUNCTIONS	60
	REFERENCES	74

LIST OF FIGURES

Figure 1.1.	Propagation of a P-Wave.	12
Figure 1.2.	Propagation of a S-wave.	13
Figure 1.3.	Propagation of a Rayleigh Wave.	13
Figure 1.4.	Propagation of a Love Wave.	14
Figure 1.5.	A Replica of Houfeng Didong Yi.	14
Figure 1.6.	Sketch of a C-Spring Seismometer.	15
Figure 1.7.	The CMG-40 TOBS Ocean Bottom Seismometer of Güralp Systems. ...	16
Figure 1.8.	Sketch of a Lehman Seismometer.	16
Figure 1.9.	An overall view (on the left) and a zoomed view to the tip (on the right) of a SG Type Seismometer.	17
Figure 1.10.	An Overall View and a Zoomed View to the Tip of the new SG Type Seismometer build by the author and M.H.Calayır together in 2004.	18
Figure 1.11.	An Overall View of the Cad Model of the new SG Type Seismometer build by M.H.Calayır G.Kakı and B.Müstecapoğlu in 2010.	18
Figure 2.1.	The Response of the Seismometer to Seismic Waves with Different Frequencies.	19
Figure 2.2.	The Position of the Pendulum in two Different Systems of Varying Frequencies.	20
Figure 2.3.	The Position of the Pendulum in the case $f_p \gg f_m$	21
Figure 2.4.	The Position of the Pendulum in the case $f_p \ll f_m$	21
Figure 2.5.	Radial Force Sketch for the Deduction of the Period of a Mathematical Pendulum.	22
Figure 2.6.	Sketch of the Magnetic Counterforce acting on the Pendulum.	23
Figure 2.7.	Sketch of the Simple Pendulum.	24
Figure 2.8.	Masked (on the left) and unmasked (on the right) Idealized (Simple) Pendulum Simulink Model.	26
Figure 2.9.	Sketch of the Simple Pendulum with Magnetic Counterforce.	26
Figure 2.10.	Masked (on the left) and unmasked (on the right) Magnetic Counterforce Simulink Model.	30

Figure 2.11.	Sketch of the Simple Pendulum with Magnetic Counterforce and with changing Air Drag Force.	31
Figure 2.12.	Masked (on the left) and unmasked (on the right) Air Drag Force Simulink Model.	33
Figure 2.13.	The Real Pendulum Kinematics Model of the new SG Type Seismometer with Magnetic Counterforce.	34
Figure 2.14.	Signal Generator Model with Simplified Pendulum Block.	36
Figure 2.15.	Transmitter Receiver System.	37
Figure 3.1.	Golden Section Search Diagram.	40
Figure 3.2.	Magnetic Counterforce Optimization Diagram (Green Blocks: Models built in Simulink; Blue Blocks: Functions and Algorithms written in Matlab; Black Block: Unnecessary and Discarded Part in Modelling). ..	43
Figure 3.3.	The Imitation of the Two of the Three Possible Cases with Desired and Current Oscillation of the Pendulum.	45
Figure 3.4.	The Imitation of the Third Case with Desired and Current Oscillation of the Pendulum.	45
Figure 3.5.	Oscillation of the Pendulum with different magnetic counterforce constant values.	46
Figure 3.6.	Magnetic Counterforce Constant Effect on Pendulum Oscillation.	47
Figure 3.7.	Oscillation Period Optimization Diagram (Green Blocks: Models built in Simulink; Blue Blocks: Functions and Algorithms written in Matlab; Black Block: Unnecessary and Discarded Part in Modelling).	48
Figure 3.8.	Error Output mapped against Magnetic Counterforce Constant.	49
Figure 3.9.	Maximum Angle Displacement Effect on Error Output.	49
Figure 3.10.	The Effect of the Change in Total Pendulum Mass on Error Output.	50
Figure 3.11.	The Effect of the Change in Total Pendulum Length on Error Output. ..	50
Figure B.1.	Real Pendulum Kinematics Model of the new SG Type Seismometer with Magnetic Counterforce (masked).	60
Figure B.2.	Simplified Pendulum Model for estimating the desired Theta Signal.	60
Figure B.3.	Transmitter Receiver Part Signal Processing to get the Signal $\theta(t)$ in Real Pendulum.	61

LIST OF SYMBOLS

$\alpha_i(x)$	Optimization constraints
C_B	Magnetism constant
C_D	Drag coefficient
f_m	Frequency of the moving system
f_p	Frequency of the pendulum
F_C	Magnetic counterforce
F_r	Radial force
F_R	Restoring force
T	Period of the pendulum
x_1	Magnetic counterforce constant
ϕ	Golden ratio
$I(\theta)$	Current function flowing through the coil
θ	Angular displacement of the pendulum
ω_0	Characteristic frequency of seismometer

LIST OF ACRONYMS/ABBREVIATIONS

SG Shackleford and Gundersen

1. INTRODUCTION

1.1. Seismic Waves

Seismic waves are huge energy waves that advance on the surface or inside the earth. They are caused mostly by earthquakes but also sometimes by volcanic eruptions or big explosions. The seismic waves are gathered in two groups regarding their path of travel:

- Body waves
- Surface waves

1.1.1. Body Waves

The waves that travel in the mantle or core of the earth are named as Body waves. P-waves and S-waves are in this wave group.

P-waves are pressure waves and they travel faster than all other seismic waves. Therefore they are named as Primary waves. However they are also called as Compression waves because of their propagation characteristics. The direction of vibration is the same as the direction of the wave propagation.

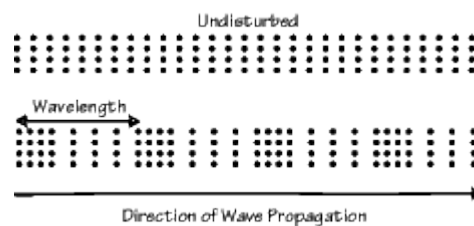


Figure 1.1. Propagation of a P-Wave [1] .

S-waves are shear waves and their motion is perpendicular to the direction of the propagation. They are slower than P-waves and arrive at the location where the seismic measurement is being done later therefore they are called as secondary waves. Their speeds are in general around 60% of the P-waves in different materials.

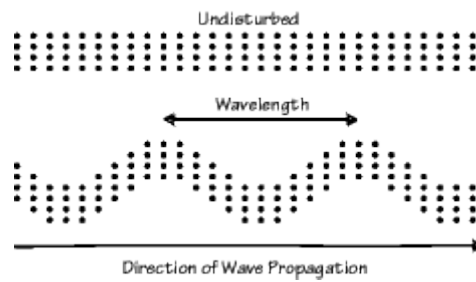


Figure 1.2. Propagation of a S-wave [1] .

The direction of wave propagation for these transverse waves is perpendicular to the motion of the ground which is caused by the wave.

1.1.2. Surface Waves

The waves that travel on the outer surface of the Earth are named as Surface waves, namely L-waves. Rayleigh waves, Love waves and Stonely waves are in this wave group. Rayleigh waves, which are also named as Ground roll, are surface waves which advance as ripples with motions. Their expansion is similar to the expansion of waves on the surface of water. However their restoring force is not gravitational like water waves but elastic.

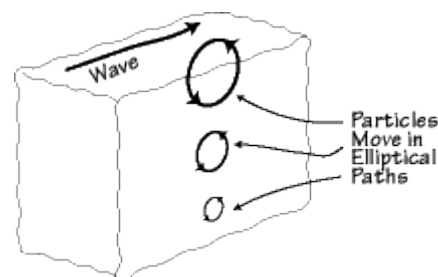


Figure 1.3. Propagation of a Rayleigh Wave [1] .

While a Rayleigh wave propagates to the right of the observer particles of inside the wave move counterclockwise in an elliptic trajectory.

Love waves are shear waves which are horizontally polarized. They vibrate the ground in the horizontal direction, perpendicular to its own direction of traveling. Love

waves are created if there exists a semi-infinite medium overlain by an upper layer of finite thickness. These dispersive waves are formed by the interaction of S waves with surface.



Figure 1.4. Propagation of a Love Wave [1] .

1.2. Detection and Measurement Methods

Earthquake is a disastrous phenomena that can't be stopped even by today's technology and knowledge. Therefore it was widely researched and studied carefully over centuries which led researchers to find different detection and/or measurement techniques of earthquakes. The focus of this thesis will be on SG type seismometers however some of the other important types of measurement techniques will be summarized here.

1.2.1. Houfeng Didong Yi

Houfeng Didong Yi is the first seismoscope that can detect an earthquake and show its direction of epicenter of the nondistant earthquakes. It was a bronze vessel with 2 meters in diameter. There were eight dragon's heads holding bronze balls around the top. If there was an earthquake, one of the mouths of the dragons would open up and drop its ball into a bronze frog sitting at the base, which makes a sound and shows the direction of the earthquakes epicenter [2] .



Figure 1.5. A Replica of Houfeng Didong Yi [2] .

1.2.2. C-Spring Seismometer

C-Spring vertical seismograph consists of a c shaped spring, a damping mechanism and a magnet with a coil acting as a sensor. It detects an earthquake by measuring the vertical distance changes between the magnet and the coil which causes to induce a current. This induced current is then amplified, passed from a low pass filter and processed in a computer to obtain the magnitude of the earthquake. The Idea of using the C-shaped spring increases the period of oscillation by enabling to use a longer spring inside a shorter height [3] .

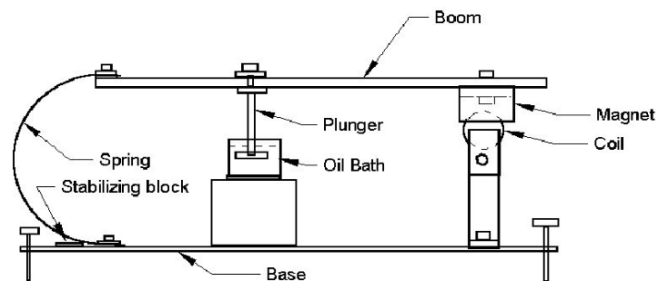


Figure 1.6. Sketch of a C-Spring Seismometer.

1.2.3. Teleseismometer

This seismometer uses levitation of diamagnetic objects to make measurements. A small proof mass is tried to be hold motionless relative to the frame by acting electrical or magnetic forces on it. The device records this force and calculates the acceleration of the mass. Therefore these devices are also called as force balance accelerometer. The displacement of earth is then calculated with algebraic calculations. Because the main measurement system consist of a small mass and electronics these type of seismometers are in general the smallest in volume which makes them ideal for placing in durable casings and take measurements on ocean bottom.



Figure 1.7. The CMG-40 TOBS Ocean Bottom Seism. build by Güralp Sytem Ltd [4] .

1.2.4. Lehman Seismometer

The Lehman Seismometer is based on a rotational system which is slightly tilted from vertical. Its connections and motion are similar to the connections and the motion of a gate therefore it is also called as the Garden Gate configuration. If degree from vertical axis was 90 degrees, it would be a simple physical pendulum. The main idea is to increase the period of the pendulum with the help of the mechanical design such that the support structure counteracts much of the gravitational force, and the component of the gravitational force which is left becomes very small. Therefore an increased period of oscillation is reached with finer mechanical adjustments.

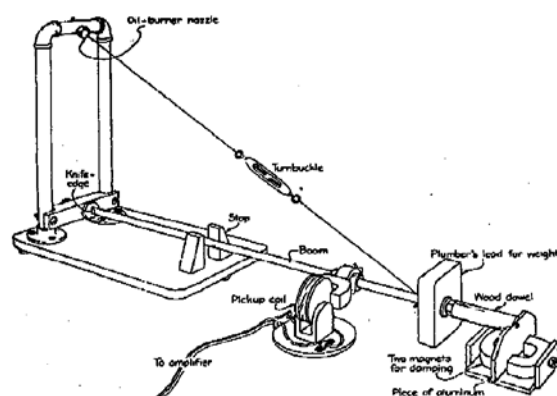


Figure 1.8. Sketch of a Lehman Seismometer [5] .

1.2.5. Shackleford Gundersen Seismometer

Shackleford Gundersen Seismometer uses a pendulum as an harmonic oscillator. The main idea behind this type of seismometers is that the location of the pendulum is read with a transmitter receiver system attached to the tip of the pendulum. This location signal is then integrated and with the help of electronic circuitry p and s waves are estimated. The mechanical design and circuitry be optimized to improve the output however the real period value of the pendulum remains still small which in particular hinders the user to make exact measurements.

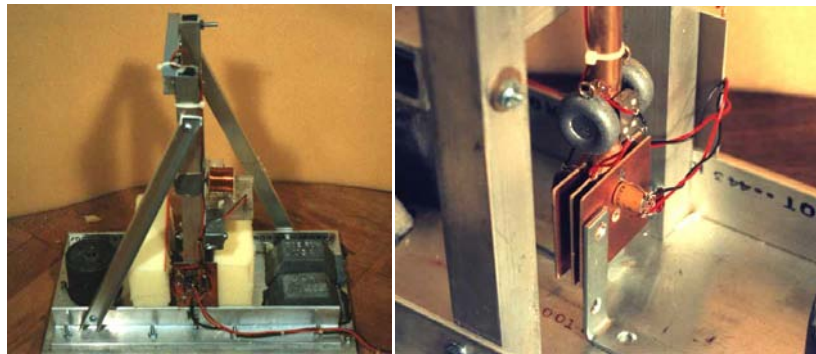


Figure 1.9. An overall view (on the left) and a zoomed view to the tip (on the right) of a SG Type Seismometer [6] .

1.3. Former Work and Past Experience

The relevant former work and past experience of the author on the topic will be explained here shortly in order to explain the work done with this thesis better. The SG Seismometer has a hinge such that by using a transmitter receiver module the exact position of the pendulum is received as a signal which is proportional to the elongation of the pendulum. While working on this seismometer system a new hinge was found by M.H.Calayir and by the author which led them to build a new SG Type Seismometer. [7] The already existing signal proportional to the elongation is amplified and given directly to the damping coil which caused a magnetic counterforce to act on the pendulum, increasing its period literally.

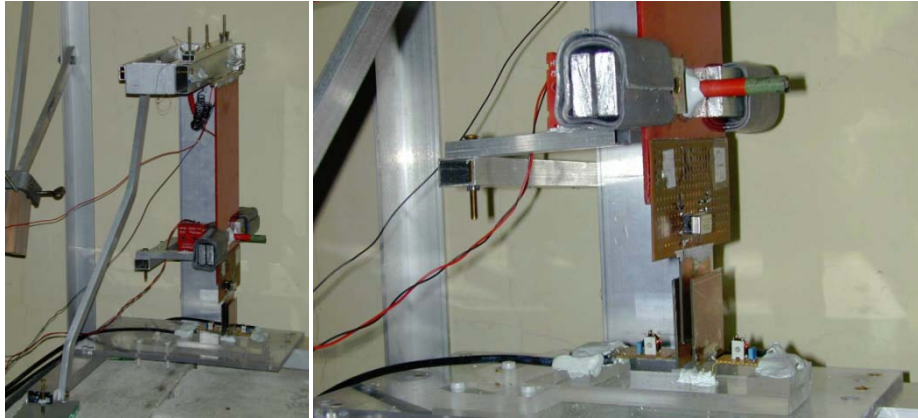


Figure 1.10. An Overall View (on the left) and a Zoomed View to the Tip (on the right) of the new SG Type Seismometer build by the author and M.H.Calayır together in 2004 [7] .

As a result of the hard work and sensitive optimization, it was proven experimentally that the magnetic counterforce method works in increasing the period because it let a period for 1.5 seconds to become 10 seconds in past experience. However it was never possible to make it increase beyond that point. The reason for that was thought to be mechanical imperfections such as not having a totally horizontal bottom plane or tip of the pendulum does not stay absolutely in the middle, or for not finding the center of gravity with enough precision, etc. However this assumption was disproved when another SG type seismometer was built by three mechanical engineers with enough mechanical perfection as shown in Figure 1.11, which didn't show any more progress in period increasing [8]. Therefore the only thing left behind was the magnetic counterforce constant so it was decided to work on it to understand the effects of its imperfection.



Figure 1.11. An Overall View of the Cad Model of the new SG Type Seismometer build by M.H.Calayır G.Kakı and B.Müstecapoğlu in 2010 [8] .

2. MATHEMATICAL AND SIMULINK MODELLING

2.1. Mathematical Model of an SG Type Seismometer

As discussed in the Introduction Part, the SG Type Seismometer that it is being modeled here, is a pendulum based seismometer. In all types of Seismometers the ultimate goal is the same which is to acquire a stable point, not affected from earth's seismic movements. This will allow this stable point to be used as a reference point such that if earth's seismic movements relative to this point is measured it will give the desired outcome. In SG and Lehman Type seismometers this stable point is achieved by using a pendulum. However all alone a normal pendulum does not give an isolated point from earth. In this case its period is increased with a magnetic counterforce proportional to the elongation of the pendulum. In order to prove the necessity of high period for the pendulum it is discussed thoroughly in the theory. Basically this seismometer consists of a pendulum with a certain characteristic frequency, ω_0 , of its own. The seismic wave is used as a driving force since the fixture of the pendulum is linked to the surface of the earth.

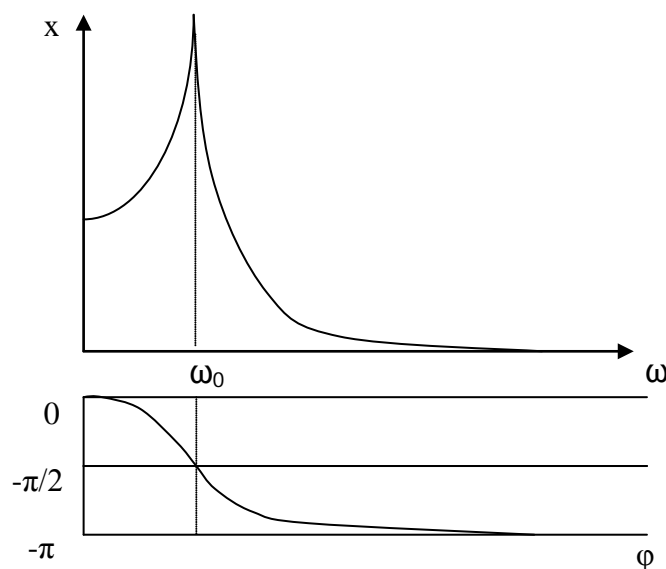


Figure 2.1. The Response of the Seismometer to Seismic Waves with Different Frequencies.

As the seismometer is intended to register the forced but not the characteristic oscillation, the characteristic frequency must be clearly lower than the forced oscillation. This can be seen in Figure 2.1, which shows the amplitude of the oscillation of the pendulum at ω_0 compared to the forced frequency ω .

There are three areas as stated below:

- $\omega_0 > \omega$: The pendulum moves in proportion to the forced oscillation with no period shift. The seismometer shows no relative movement as seen in Figure 2.3.
- $\omega_0 = \omega$: With a period shift of $\pi/2$ the pendulum is caused to resound. The resonance of the pendulum, and not the movement of the earth, is measured.
- $\omega_0 < \omega$: The amplitude of the pendulum becomes almost non-existent for the static observer. However, a dynamic observer moving with the seismic wave sees the movement of the seismic wave as a movement of the pendulum at a period shift of π as seen in Figure 2.4.

This means that the characteristic frequency of the pendulum has to be smaller than the forced frequency of the seismic wave. In order to be able to measure seismic waves of the 1 Hz – which is typical of distant waves – one needs to reach a period of 20s. However according to Equation 2.11 this would make a pendulum length of 100 meters necessary.

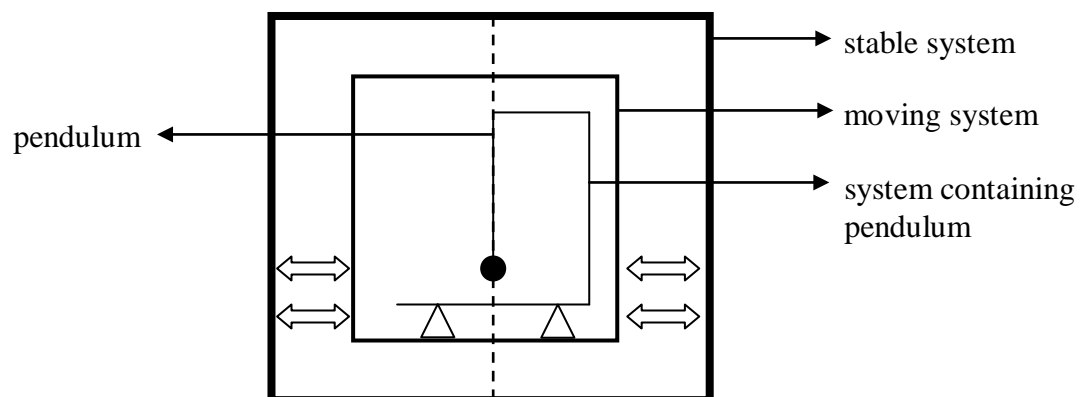


Figure 2.2. The Position of the Pendulum in two Different Systems of Varying Frequencies.

Two different systems are explained below with changing frequency of the moving system, stated as f_m , and with changing frequency of pendulum, stated as f_p .

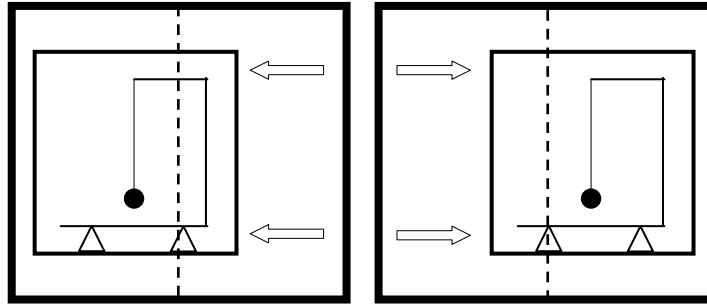


Figure 2.3. The Position of the Pendulum in the case $f_p \gg f_m$.

As seen in Figure 2.3 if $f_p \gg f_m$ is true then the pendulum moves in the same way as the moving system. Despite appearing stable within the moving system, the pendulum moves together with the stable system.

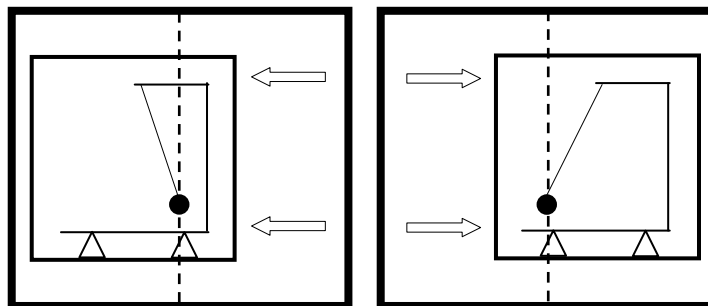


Figure 2.4. The Position of the Pendulum in the case $f_p \ll f_m$.

As seen in Figure 2.4 if $f_p \ll f_m$ is true then despite appearing to sway within the moving system, the pendulum remains stable according to the stable system. [7]

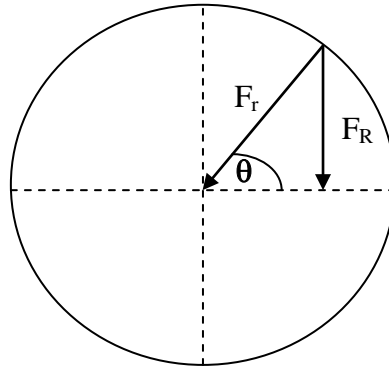


Figure 2.5. Radial Force Sketch for the Deduction of the Period of a Mathematical Pendulum.

F_r is the radial force.

$$F_r = m\omega^2 r \quad (2.1)$$

The restoring force can be found as

$$F_R = F_r \sin \theta = F_r \frac{y}{r} = m\omega^2 r \frac{y}{r} = m\omega^2 y \quad (2.2)$$

$$F_R = m \left(\frac{2\pi}{T} \right)^2 y = m \frac{4\pi^2}{T^2} y \quad (2.3)$$

which implies

$$T^2 = m \frac{4\pi^2}{F_R} y \quad (2.4)$$

$$T = 2\pi \sqrt{\frac{my}{F_R}} \quad (2.5)$$

as the first statement [7].

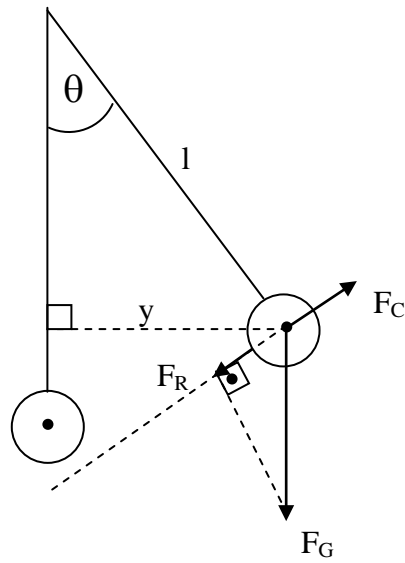


Figure 2.6. Sketch of the Magnetic Counterforce acting on the Pendulum.

If α is very small¹ then the restoring force is also equal to $\sin(\theta)$ multiple of the gravitational force.

$$F_R = F_G \sin \theta . \quad (2.6)$$

Considering

$$F_G = mg \quad (2.7)$$

and

$$\sin \theta = \frac{y}{l} \quad (2.8)$$

restoring force formula becomes

$$F_R = mg \frac{y}{l} . \quad (2.9)$$

Putting Equation 2.9 in Equation 2.5 gives out the period formula [7] as

¹ The magnitude of the period error caused by this assumption is calculated in the Appendix A.

$$T = 2\pi \sqrt{\frac{my}{mg \frac{y}{l}}} \quad (2.10)$$

$$T = 2\pi \sqrt{\frac{l}{g}}. \quad (2.11)$$

2.1.1. Mathematical Model of the Simple Pendulum (Force Derivation)

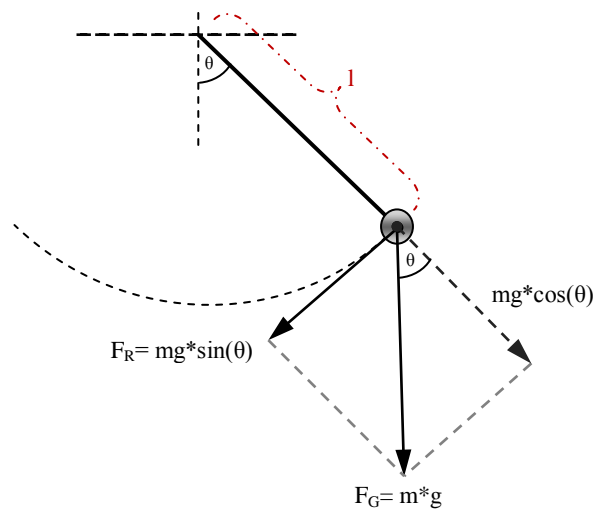


Figure 2.7. Sketch of the Simple Pendulum.

A simple pendulum can be modeled as a string, with length l , attached with a mass of m on its lower tip. As the pendulum starts its motion a restoring force F_R proportional to length l , mass m , gravitational acceleration g and angular displacement θ , acts on it as

$$F_R = -mg \sin \theta. \quad (2.12)$$

The minus sign in the equation implies that the force created by earth's gravitational force has the opposite direction then the angular displacement θ . If Newton's second law

$$F = ma \quad (2.13)$$

is considered, the expression which shows that the acceleration of the simple pendulum can easily be found as

$$-mg \sin \theta = ma \quad (2.14)$$

$$a = -g \sin \theta . \quad (2.15)$$

A second expression of pendulums acceleration regarding its movement along the arc can also be found with the help of arc length formulas which are

$$s = l\theta \quad (2.16)$$

$$v = \frac{ds}{dt} = l \frac{d\theta}{dt} \quad (2.17)$$

$$a = \frac{d^2s}{dt^2} = l \frac{d^2\theta}{dt^2} \quad (2.18)$$

So combining both expressions of acceleration, Equation 2.15, and the mathematical model of simple pendulum, Equation 2.18, gives out

$$\frac{d^2\theta}{dt^2} = -\frac{g}{l} \sin \theta \quad (2.19)$$

$$\frac{d^2\theta}{dt^2} + \frac{g}{l} \sin \theta = 0 \quad (2.20)$$

which is the mathematical representation of this simple pendulum.

2.1.2. Simulink Model of the Simple Pendulum

Simulink blocks are used to model the idealized (simple) pendulum. The model takes in g , l and initial angular position of the pendulum in radians and gives out θ , $\dot{\theta}$, $\ddot{\theta}$. This simulink model of simple pendulum will also be used in modeling the real pendulum with magnetic counterforce model. Therefore the model takes in the current $\ddot{\theta}$ value in every step as an input.

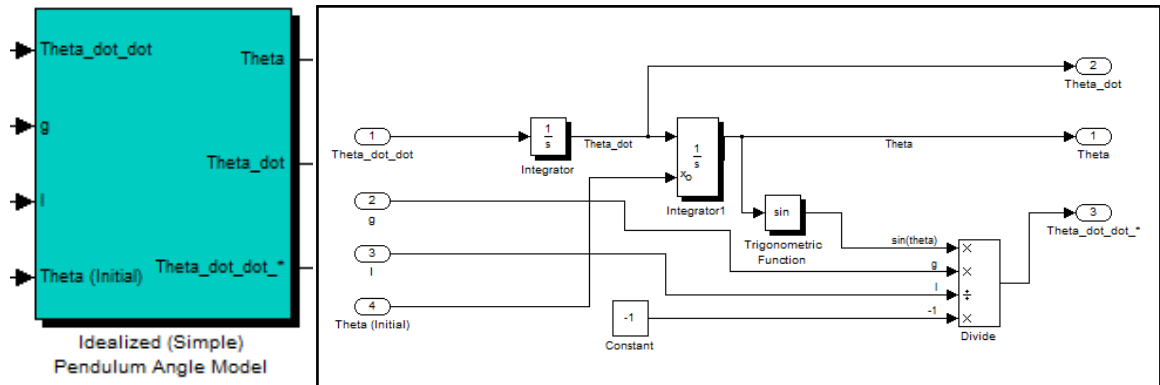


Figure 2.8. Masked (on the left) and unmasked (on the right) Idealized (Simple) Pendulum Simulink Model.

For simulating the simple pendulum model by its own the $\ddot{\theta}$ input port needs to be supplied with its own $\ddot{\theta}$ output port.

2.1.3. Mathematical Model of Magnetic Counterforce

As explained in the introduction section, the period of the pendulum needs to be increased in order to be able to make seismic measurements. By examining Equation 2.11 which is derived for period, the impression is that in order to increase the period either the length of the pendulum needs to be increased or the gravitational acceleration needs to be decreased without reaching the zero value. Increasing length will increase the period but in order to reach the required period values one must reach lengths over hundred meters, which is not feasible to build.

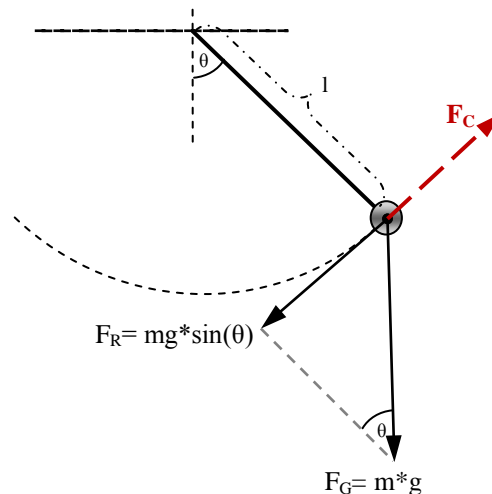


Figure 2.9. Sketch of the Simple Pendulum with Magnetic Counterforce.

The second option, decreasing gravitational acceleration, might seem unachievable in the first look, because g is dependent only to the distance of the pendulum to the Earth's center. However there is an easy way to do this if that is considered to be done "locally", which means on the pendulum only. A counterforce, F_C , can be build which will act on the pendulum with almost the same magnitude but with opposite direction of F_R . So the effect of the restoring force acting on the pendulum will decrease dramatically and the period of the pendulum will increase. This force needs to be created and driven also in the force model in order to get the new mathematical equation of the pendulum. So after adding this counterforce F_C the pendulum model becomes

$$F_R(\theta) + F_C = ma . \quad (2.21)$$

Writing down already known restoring force gives out the new pendulum model with magnetic counterforce as

$$-mg \sin \theta + F_C = ma . \quad (2.22)$$

In order to be able to solve this equation, F_C is needed to be solved first.

The magnetic counterforce is created in three simple steps. A bar magnet is fixed on the pendulums center of gravity and a coil is positioned such that the bar magnet swings inside the coil. Then a current I passes through this coil to build a magnetic field which will create a magnetic force acting on the bar magnet, that becomes the desired magnetic counterforce. This magnetic counterforce can be altered by changing the current on the coil.

$$F_C = m_p B \cos \alpha \quad (2.23)$$

where m_p is the pole strength of the bar magnet, B is the magnetic field inside the solenoid and α is the angle of the bar magnet with the magnetic field lines which is equal to θ (very near to zero), since the bar magnet is almost parallel to the magnetic field lines at zero state.

Pole strength, m_p , of the bar magnet depends on the cross-sectional area A and magnetization M of the bar magnet as

$$m_p = MA = M\pi r^2 . \quad (2.24)$$

Magnetic field B inside the solenoid is given below where μ_0 is the permeability of the free space, N is the number of turns, l_s is the length of the solenoid and I is the total current.

$$B = \mu_0 \frac{N}{l_s} I . \quad (2.25)$$

So if Equation 2.24 and Equation 2.25 is written in Equation 2.23 the magnetic counterforce becomes as

$$F_C = M\pi r^2 \mu_0 \frac{N}{l_s} I \cos \theta \quad (2.26)$$

The restoring force is changing proportional to the elongation if θ is small, which is true in this case. Therefore the magnetic counterforce should also change almost proportional to the elongation which can be assured by changing the current I proportional to the elongation. It means that $I = I(\theta)$ and the counterforce becomes

$$F_C(\theta) = \underbrace{M\pi r^2 \mu_0 \frac{N}{l_s}}_{C_B} I(\theta) \cos \theta . \quad (2.27)$$

As $M\pi r^2 \mu_0 \frac{N}{l_s}$ is not changing they all can be summed up inside a new constant C_B , which will be called as the magnetism constant of the seismometer in this thesis, as

$$C_B = M\pi r^2 \mu_0 \frac{N}{l_s} \quad (2.28)$$

which leads the magnetic counterforce to become

$$F_C(\theta) = C_B I(\theta) \cos \theta . \quad (2.29)$$

Current $I(\theta)$ is proportional to the elongation. Therefore it can also be written as

$$I(\theta) = x_1 \theta + x_0 \quad (2.30)$$

It is known that while pendulum is at its starting position ($\theta = 0 \text{ rad}$) no magnetic counterforce should be exerted on it. Therefore it can easily be found by simple mathematic that $x_0 = 0$ and the current function is reduced to

$$I(\theta) = x_1 \theta . \quad (2.31)$$

So the magnetic counterforce function becomes

$$F_C(\theta) = C_B x_1 \theta \cos \theta \quad (2.32)$$

where x_1 is the magnetic counterforce constant and C_B is magnetism constant.

Equation 2.32 placed in Equation 2.22 gives out

$$ma = -mg \sin \theta + C_B x_1 \theta \cos \theta . \quad (2.33)$$

which implies

$$a = -g \sin \theta + \frac{C_B}{m} x_1 \theta \cos \theta \quad (2.34)$$

$$l \frac{d^2 \theta}{dt^2} = -g \sin \theta + \frac{C_B}{m} x_1 \theta \cos \theta \quad (2.35)$$

$$\frac{d^2 \theta}{dt^2} = -\frac{g}{l} \sin \theta + \frac{C_B}{m * l} x_1 \theta \cos \theta . \quad (2.36)$$

2.1.4. Simulink Model of Magnetic Counterforce

Equation 2.36 gives out the mathematical model of the pendulum affected with the magnetic counterforce. It is easy to see that it consists of two parts. First part is already found to be the simple pendulum model part as

$$\frac{d^2\theta}{dt^2} = -\frac{g}{l} \sin \theta . \quad (2.37)$$

It is added up with a θ dependant new part, which is $\frac{C_B}{ml} x_1 \theta \cos \theta$. Therefore it is possible to build this magnetic counterforce model as an addition to the simple pendulum model in simulink which will make the real SG type pendulum model more flexible.

The sub-model takes in θ , $I(\theta)$, C_B , m , l and gives out the addition to $\ddot{\theta}$ of the simple pendulum model.

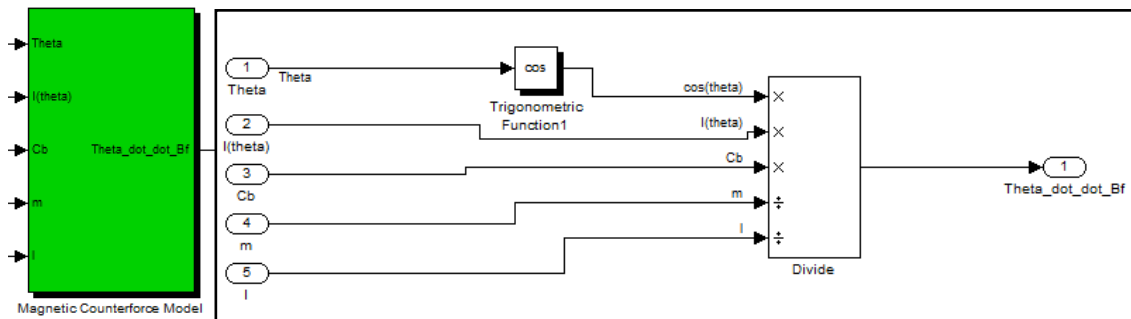


Figure 2.10. Masked (on the left) and unmasked (on the right) Magnetic Counterforce Simulink Model.

One more thing to worth mentioning here is that by looking the mathematical and simulink model of magnetic counterforce one can be misled to the assumption that the length in the magnetism constant and the length in this model should cancel each other which means that they are redundant. However they are not the same lengths where the former is the length of the coil and the latter is the length of the pendulum therefore both of them are required inside the model.

2.1.5. Mathematical Model of Air Drag Force

Air drag force model is another part of the real pendulum model which has been seen as negligible by past self experience but in order to simulate its real affects this model is also built.

In order to build this model the magnitude and direction change of the force component needs to be figured out which is being created as the air drag force in the dependence of θ . As it is explained before the pendulum in this system moves only in two directions assuming to be a thin rectangular prism, or better to say a flat plate, moving with its big surface against air resistance.

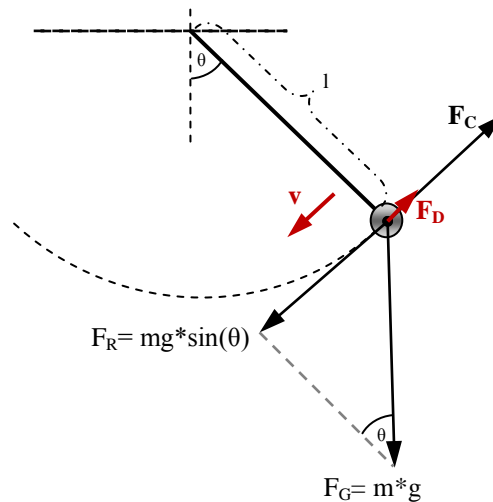


Figure 2.11. Sketch of the Simple Pendulum with Magnetic Counterforce and with changing Air Drag Force.

The air drag force [9] is calculated as

$$\vec{F}_D = -\frac{1}{2} \rho \vec{v}^2 C_D A . \quad (2.38)$$

The minus sign in this equation clearly implies that the drag force created by air resistance has the opposite direction then the speed vector \vec{v} . ρ is the density of air, C_D is the drag coefficient of pendulum in its direction of motion and A is the reference area perpendicular to the direction of motion. If this drag force equation is added to the real pendulum force model becomes

$$m\vec{a} = \vec{F}_R(\theta) + \vec{F}_C(\theta) + \vec{F}_D(\vec{v}) \quad (2.39)$$

$$= -mg \sin \theta + C_B x_1 \theta \cos \theta + \vec{F}_D(\vec{v}) \quad (2.40)$$

$$= -mg \sin \theta + C_B x_1 \theta \cos \theta - \frac{1}{2} \rho \vec{v}^2 C_D A. \quad (2.41)$$

Reminding back to Equation 2.18 and Equation 2.17, the equation above also implies that

$$\frac{d^2\theta}{dt^2} = -\frac{g}{l} \sin \theta + \frac{C_B}{ml} x_1 \theta \cos \theta - \frac{\rho \vec{v}^2 C_D A}{2ml} \quad (2.42)$$

$$\frac{d^2\theta}{dt^2} = -\frac{g}{l} \sin \theta + \frac{C_B}{ml} x_1 \theta \cos \theta - \frac{\rho l C_D A}{2m} \left(\frac{d\theta}{dt}\right)^2. \quad (2.43)$$

2.1.6. Simulink Model of Air Drag Force

Equation 2.43 gives the mathematical model of the simple pendulum with magnetic counterforce and with air drag force. It is again easy to see that it has the pendulum with magnetic counterforce model

$$\frac{d^2\theta}{dt^2} = -\frac{g}{l} \sin \theta + \frac{C_B}{ml} x_1 \theta \cos \theta \quad (2.44)$$

added up with a velocity dependent part

$$\frac{\rho l C_D A}{2m} \left(\frac{d\theta}{dt}\right)^2 \quad (2.45)$$

therefore it is again possible to build this air drag force model as an addition to the pendulum with magnetic counterforce model in simulink. The sub-model takes in ρ , l , C_D , A , m , and velocity \vec{v} and gives out the addition to $\ddot{\theta}$ of the simple pendulum model. The air drag force model shown in Figure 2.12 is highly dependent on the drag coefficient C_D because it is not possible to find a general coefficient. As the shape of the pendulum and its attachments on the swinging part changes the drag coefficient will change accordingly. In

order to solve this uncertainty the worst case is assumed and the C_D of a flat plate is used, which is even greater than the C_D of an upright positioned human [9].

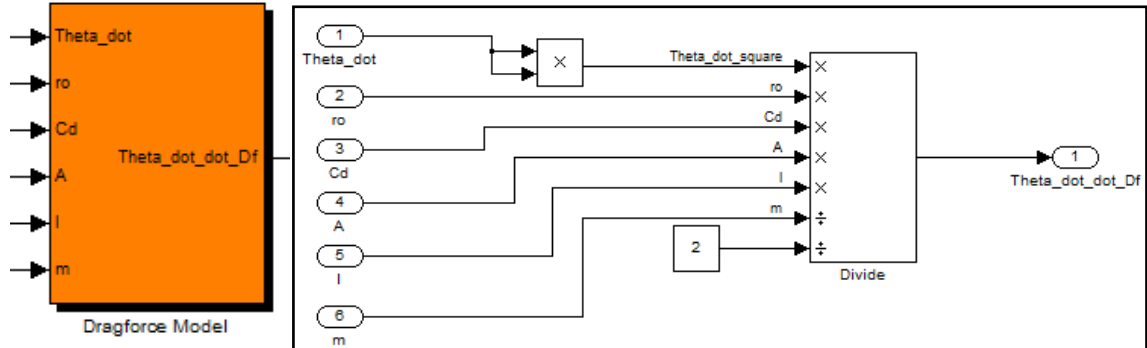


Figure 2.12. Masked (on the left) and unmasked (on the right) Air Drag Force Simulink Model.

2.1.7. Simulink Model of the Real Pendulum with Magnetic Counterforce

Until now all major sub-blocks needed to build the Real Pendulum Kinematic Model is created in simulink. The last step is summing them up together by building the necessary connections.

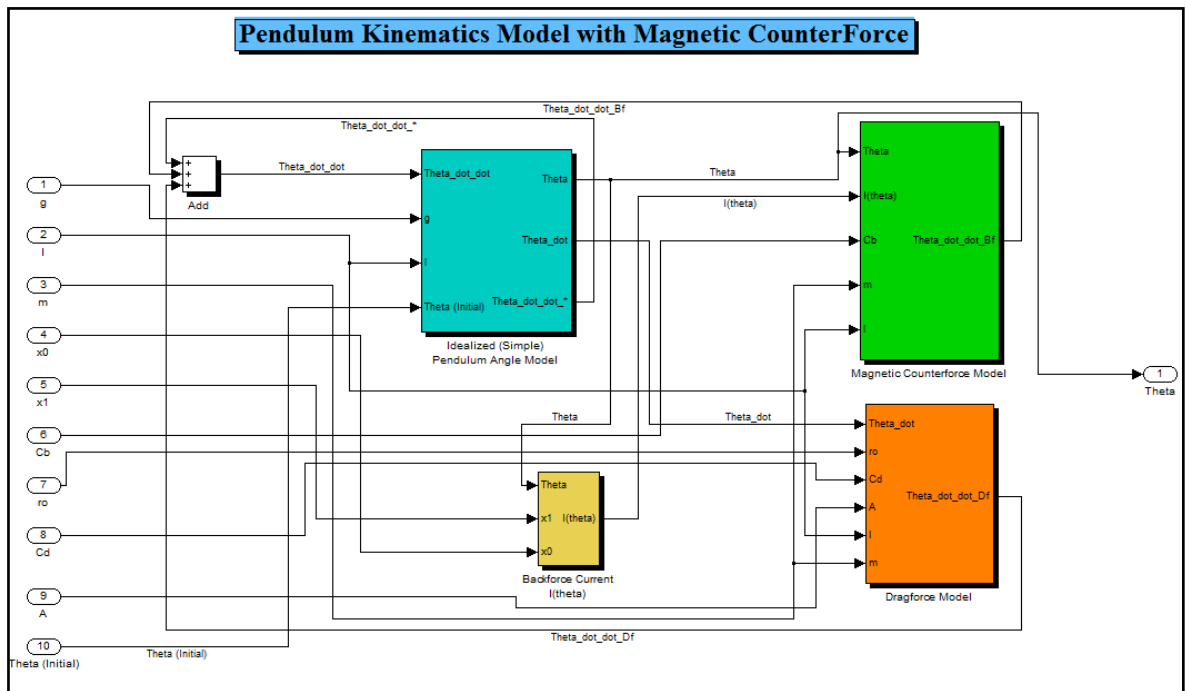


Figure 2.13. The Real Pendulum Kinematics Model of the new SG Type Seismometer with Magnetic Counterforce.

$I(\theta)$ is actually found to have only one nonzero coefficient, namely x_1 , therefore its sub-model becomes redundant but it is not discarded and kept inside the model for future work.

The model is masked as seen in Figure B.1. It takes all necessary constants and variables which are g , l , m , x_0 , x_1 , C_B , C_d , A , and θ (initial) and gives out only its angular position, namely θ . However this sub-model is built as it uses θ in radians. Therefore also radians to degrees and degrees to radians converters are built on both inside and outside ports of θ which made it more convenient to work with theta in degrees.

2.2. Other Required Models

2.2.1. Signal Generator 1

This simulink block is built in order to create the signal with a desired period. It does not need to be real. The most important requirement for this signal is that it should give out

an harmonic oscillation which can be altered by changing the initial magnetic counterforce constant. Therefore a simplification has been made such that the oscillation becomes an harmonic oscillation by using the fact that the angle θ is very small. Equation 2.46 gives the oscillation of a pendulum with magnetic counterforce as below.

$$ma = -mg \sin \theta + M\pi r^2 \mu_0 \frac{N}{l_s} x_1 \theta \cos \theta \quad (2.46)$$

As explained above by considering the fact that $\theta \ll 1$, $\cos \theta$ is simplified as 1, $\sin \theta$ is simplified as θ and all constants multiplied with x_1 are also summed up as C_B . These simplifications changes Equation 2.46 as

$$a = -g\theta + C_B x_1 \theta. \quad (2.47)$$

Considering Equation 2.18 the model reduces to

$$l \frac{d^2 \theta}{dt^2} = -g\theta + C_B x_1 \theta \quad (2.48)$$

$$\frac{d^2 \theta}{dt^2} = -\frac{g}{l} \theta + \frac{C_B}{l} x_1 \theta \quad (2.49)$$

$$\frac{d^2 \theta}{dt^2} = -\frac{g - C_B x_1}{l} \theta. \quad (2.50)$$

The mathematical representation of simple harmonic oscillation is given in the following equation [10]:

$$\frac{d^2 x}{dt^2} = -\frac{k^*}{m^*} x. \quad (2.51)$$

As seen above the simplified system has a harmonic oscillation form with

$$k^* = g - C_B x_1 \quad \text{and} \quad m^* = l$$

The period of this simplified pendulum is found with the formula [10]:

$$T = 2\pi \sqrt{\frac{m^*}{k^*}}. \quad (2.52)$$

In this simplified case it becomes

$$T = 2\pi \sqrt{\frac{l}{g - C_B x_1}}. \quad (2.53)$$

For a given period value, an approximated x_1 value can be calculated such that it allows the simplified pendulum model to create the desired harmonic oscillation signal.

$$x_1 = \left(g - \frac{4\pi^2 l}{T_{des}^2} \right) \frac{1}{C_B} \quad (2.54)$$

As explained above this is not the simple (idealized) pendulum model or not the real pendulum model. They are already stated in Equation 2.19 and in Equation 2.36 correspondingly. This simplified model is used only by creating a reference signal with any given desired period length for error calculation. The mathematical representation is modelled and masked as seen in Fig. 2.14. Inside the mask is also given in Figure B.2.

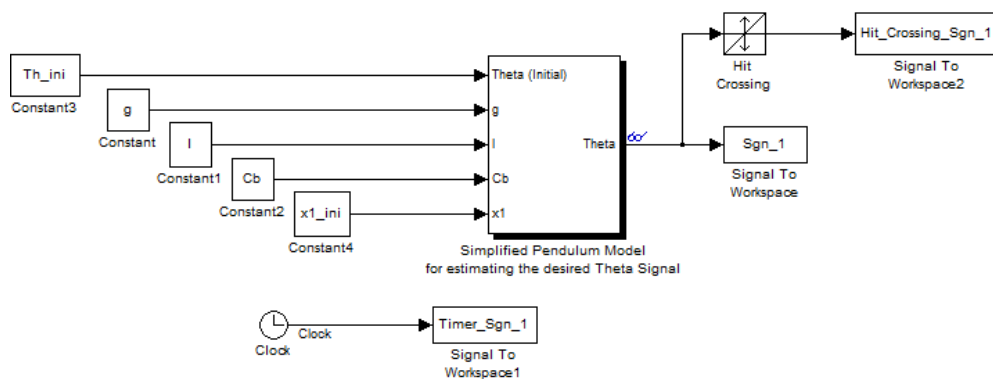


Figure 2.14. Signal Generator Model with Simplified Pendulum Block.

After defining its already known characteristics (mass, length, etc.) the model needs only two inputs. First one is the θ_{ini} which is the starting angle displacement of the pendulum. This input is of course choice dependent and comes in as an initial statement.

The second input is the x_{1_ini} which is the magnetic counterforce constant for the “Simplified Pendulum Model” to oscillate with the desired period value.

2.2.2. Signal Generator 2

This model is a simple sinusoidal signal generator block with the given mathematical representation in Equation 2.55 below as

$$f(t) = a * \cos(bt + c) . \quad (2.55)$$

The required variables a, b and c are calculated with the matlab function “Variable Calculation” which will be explained thoroughly in the next chapter.

2.2.3. Transmitter Receiver model

This is the part of the Seismometer, attached to the tip of the pendulum, measuring the elongation of the pendulum as θ .

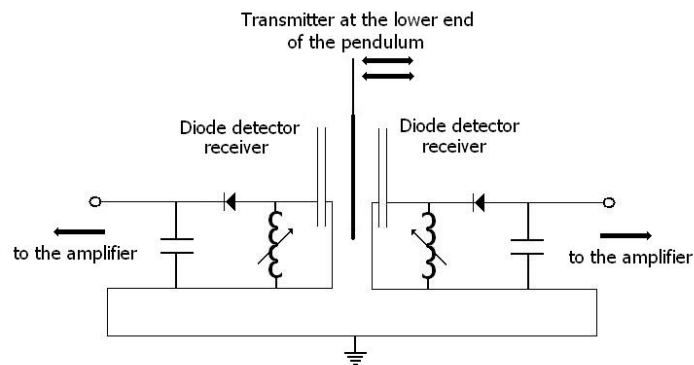


Figure 2.15. Transmitter Receiver System [7] .

Shackleford and Gunderson were first to use AM-radio technology to learn the pendulums exact position in Seismometers. It functions by taking the advantage of the fact that the strength of the signals received depends on the distance between the transmitter and the receiver, which is attached to the lower tip of the pendulum. A graphical representation of how this part of the seismometer works is given in Appendix B. However this model is discarded and not built in simulink because it is redundant. It only takes in θ

from the real pendulum model and gives out the same value, namely θ . The only effect this model causes is a small time delay which can be calculated as following. The distance between receiver and transmitter plates is at most 3mm in this case. Therefore radio waves travelling from the transmitter to the receiver will cause the delay calculated below.

$$Delay = \frac{3mm}{c} = \frac{0,003m}{299792458m/s} \approx 10^{-11}s = 10 \text{ pico seconds} .$$

This delay of ca. 10 picoseconds is smaller than the resolution of the simulation therefore this model becomes redundant and left out of the thesis.

3. OPTIMIZATION

3.1. Theoretical Background

This section will start with an introduction of the general optimization problem subject to constraints. Then two solution methods of optimization which play an important role in this thesis will be mentioned by explaining in detail of how they are implemented. General optimization problem subject to constraints is formulated as in Equation 3.1 below.

$$\begin{aligned} & \min f(x) \\ \text{s.t. } & a_i(x) = 0, \quad i \in E \\ & a_i(x) \geq 0, \quad i \in I \end{aligned} \tag{3.1}$$

The function $f(x)$ is called here the cost function. The constraints $a_i(x)$'s for $i \in E$ are equality constraints and $a_i(x)$'s for $i \in I$ are inequality constraints. Both $f(x)$ and $a_i(x)$'s can be linear, non-linear, convex or non-convex. Moreover $f(x)$ can be quadratic or non-quadratic. It is assumed here that the reader has the fundamental knowledge of these terms in optimization theory. These properties bring the following problem classifications in optimization.

- If $f(x)$ and $a_i(x)$'s are convex, then it is called a convex problem and the local minimum is also the global minimum.
- If $f(x)$ and $a_i(x)$'s are linear, then the problem is called linear programming and the solution is rather simpler than the nonlinear case.
- If $f(x)$ is in quadratic form and $a_i(x)$'s are linear, then it is called a quadratic programming problem, which again is rather simple to solve.

The optimization problems are solved in an iterative way, where the solution is approached one step at a time on ever iteration [11,12].

3.1.1. Binary search method

The binary search method is an optimization algorithm which finds the location of a specified target within a search interval. In every step the algorithm goes to the middle point and checks the target value against this current value. If the values are the same or their difference is below a predetermined threshold τ then the algorithm decides that it has reached the target. If the current value is smaller or bigger than the target value then the algorithm halves its search interval by throwing the corresponding unnecessary half of the interval out. This process is repeated until the remaining interval is narrowed below the threshold value τ if the first statement is never fulfilled [13].

This algorithm can be applied as recursive or iterative. In recursive method the algorithm calculates the midway point of the initial interval, determines which of the two subintervals to search, and then does a recursive call to search that subinterval. In iterative method the algorithm runs a loop where it progressively narrows the search interval and jumps out of the loop if it finds its target value. In this thesis the latter method is used by building the binary search algorithm.

3.1.2. Golden section search method

The golden section search method is an optimization technique to approach to the minimum or maximum point of a unimodal function. In this technique the search interval is successively narrowed until it becomes smaller than a predetermined resolution factor.

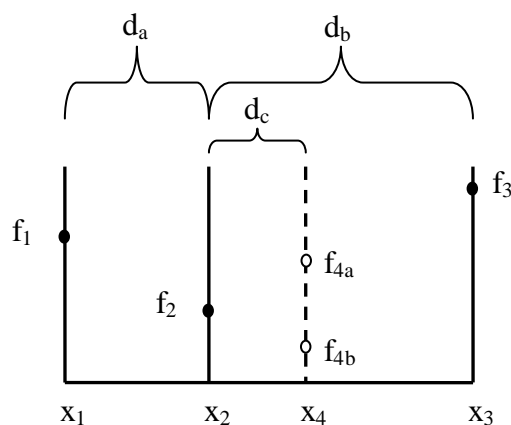


Figure 3.1. Golden Section Search Diagram.

The method is named after the fact that it maintains the function values of three points whose distances form a golden ratio. In every iteration the algorithm has three points and its function values. Two of them are boundary condition (x_1, x_3) and the third one is the golden section point calculated in the previous iteration (x_2). In order for x_2 to be the golden section of the initial boundary statement

$$\frac{d_b}{d_a} = \phi \quad (3.2)$$

must hold where ϕ is the golden ratio. The next iteration point must also fulfill the same statement. It is done by choosing the fourth point as:

$$x_4 = x_1 + (x_3 - x_2) \quad (3.3)$$

This new point replaces one of the boundary condition points regarding its function output. In the above example it replaces x_3 for the f_{4a} output case and x_1 for the f_{4b} output case. These iterations continue until the termination condition is met. There are many different termination conditions. It is important to pick and alter the termination condition correctly in order to be sure that the algorithm gives the correct desired output in all cases. The simplest termination condition is to check the size of the search interval in every iteration and terminate the algorithm if it gets below a certain value, τ [13].

3.2. Problem Definition

In the previous chapter a real pendulum model is defined in simulink. The goal here is to increase the pendulums period up to a desired high value. In previous attempts, which are explained in the first chapter, it was proven experimentally that the magnetic counterforce method works in increasing the period because it let a period for 1,5 seconds to become 10 seconds in past experience. However it was never possible to make it increase beyond that point [7]. The reason for that was thought to be mechanical imperfections such as not having a totally horizontal bottom plane or tip of the pendulum does not stay absolutely in the middle, or the center of gravity of the pendulum is not found with enough precision, etc. However this assumption was disproved when another SG type

seismometer was built by three mechanical engineers with enough mechanical perfection [8]. The only thing left behind was the magnetic counterforce constant so it was decided to work on it to understand the effects of its imperfection.

The two important characteristics already known about the effects of counterforce constant are that increasing it from zero starts increasing the period and increasing it beyond the point that it beats up the gravitational force it starts preventing the pendulum to continue its harmonic oscillation. Therefore the aim here is to prove in simulation that any mechanically robust SG Seismometer could be improved such that its period value goes over twenty seconds without its harmonic oscillation being disrupted.

3.3. Solution Approach

It is explained in the second chapter that a simulink model of the real SG type seismometers pendulum needs to be created in order to achieve this goal. Also an optimized counterforce constant needs to be found for any given reasonable value for seismometer characteristics. Therefore an optimization code should also be prepared such that it uses some optimization techniques to converge to a magnetic counterforce constant value for every desired period value after a finite number of iterations which ensures the pendulum to have an harmonic oscillation with a desired high period value. This goal is reached in two steps. In the first step an algorithm is built such that it can converge to a magnetic counterforce constant value for a given period value. In the second step this optimization algorithm supplies a second optimization algorithm which uses the first one repeatedly in every step in finding the magnetic counterforce constant and converges to a period value by checking the output oscillation for being a harmonic oscillation.

3.3.1. Magnetic Counterforce Optimization

In this part and in the following parts it will be explained how matlab is used to create the environment with simulink blocks, mentioned in the previous chapter, and how it is used to run necessary simulations. The real pendulum with magnetic counterforce model gives only one output which is the degree of displacement of the pendulum, namely θ . This is true because with a real SG type seismometer there is no access to any other

variable while it is working. This θ actually comes through the Transmitter Receiver Module which is explained entirely in the second chapter. In this model it is captured and filled to a dataset with corresponding time points. This dataset, full of θ values, needs to be visualized such that it shows the properties of the oscillation. Also the current period value of the oscillation needs to be calculated in order to supply the optimization algorithm with this vital information. Therefore a signal needs to be created and its period needs to be calculated simultaneously.

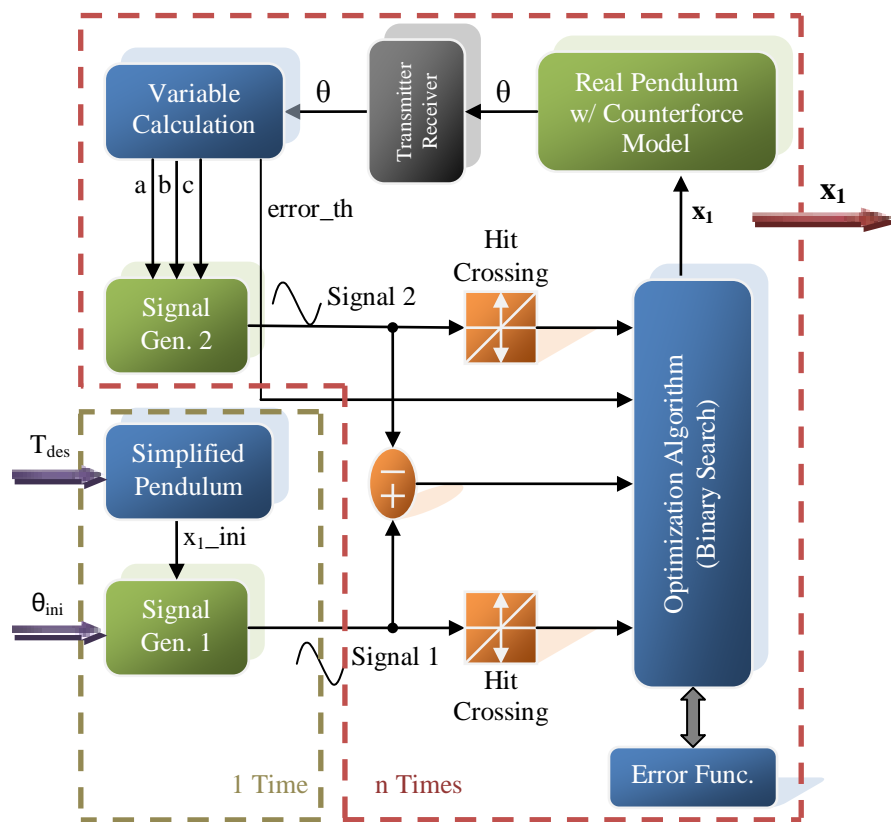


Figure 3.2. Magnetic Counterforce Optimization Diagram (Green Blocks: Models built in Simulink; Blue Blocks: Functions and Algorithms written in Matlab; Black Block: Unnecessary and Discarded Part in Modelling).

The pendulum of the seismometer makes in its natural state a harmonious oscillation which can be modeled as a sinusoidal signal. A signal generator simulink model is built with simplification and speed optimization for this purpose only, which is explained in the previous chapter as a simulink block. In order to create the signal the model needs the corresponding parameters referred as a, b and c. For this purpose a matlab function

“Variable Calculation” is created. It calculates the required amplitude, frequency and phase of the signal with the given algorithm in appendix C. However it was later understood that these outputs are not enough for this step. In the case that the magnetic counterforce becomes too powerful the oscillation of the pendulum is hindered. The tip of the pendulum never crosses the zero point and makes to the other half. Instead it is pulled or pushed with such a big counterforce such that it never completes a full swing. Therefore this matlab function also checks whether the signal crosses zero, and raises a flag correspondingly. So with these inputs the simulink block “Signal Generator 2” creates the signal visualizing the oscillation of the pendulum.

In order to compare the current period of the signal with the desired period value another signal with the desired period needs to be created. This process needs to be done for ones in every cycle because the desired signal does not change in every step. It is stored and used over and over again in calculating the error. The simulink block creating this desired signal is derived from the simplified pendulum model. After defining its already known characteristics (mass, length, etc.) it needs only two additional inputs. First one is the θ_{ini} which is the starting angle displacement of the pendulum. This input is of course choice dependent and comes in as an initial statement. The second input is the x_{1_ini} which is the magnetic counterforce constant for the simplified pendulum model to oscillate with the desired period value. This input is calculated with the matlab function “simplified pendulum” and fed to the simulink block.

The optimization algorithm improves magnetic counterforce constant in every iteration until it reaches to the given resolution, namely τ . The most important part here is the error function algorithm. In every iteration it only takes in hit crossings of both signals, the difference of the two signals and the error flag of variable calculation function. After visualizing both signals it was decided to use only one fourth of the period of the signals for error calculation. This allows sparing a great amount of computational power by itself. It also simplifies the error function algorithm by reducing the possible cases with two signals down to three cases which reduces the computational power need of the algorithm. These three possible cases are shown in the Figure 3.3 and Figure 3.4. In the first two cases both signals are created for the time interval one fourth of their own period length. The only difference is that in the former case the desired signals period is greater than the

current signals period and in the latter case it is vice versa. In these both cases the error function runs until one of the signals hits zero. It measures the size of the difference area between them and divides it to the corresponding time length.

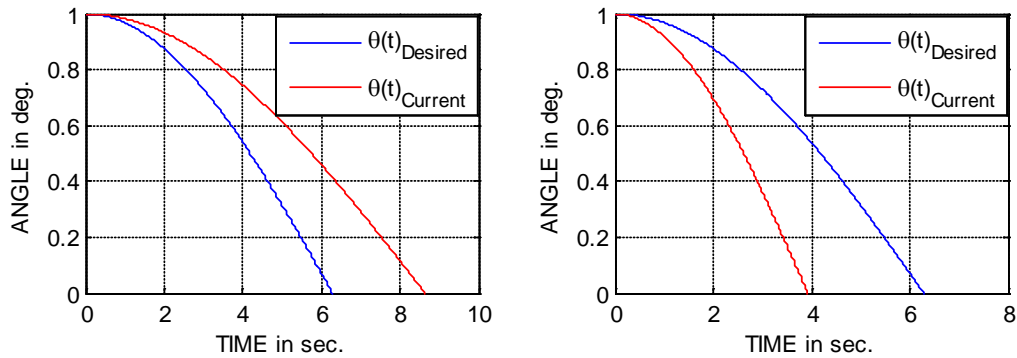


Figure 3.3. The Imitation of the Two of the Three Possible Cases with Desired and Current Oscillation of the Pendulum.

This division to time ensures that the error function becomes independent of the time interval that passes until the first zero hit of the signals and also it ensures that larger period values create reduced error output if compared to smaller period values. The third case in Figure 3.4 is different than the first two. In this case the current oscillation never reaches zero. This happens if the magnetic counterforce grows beyond a certain value and it obviously tells the algorithm to reduce the magnetic counterforce constant. Therefore for this case a flag is built to be raised in variable calculation function. The optimization algorithm checks this flag once in every iteration and if it is raised, it gives out the maximum negative error which allows the magnetic counterforce constant to be reduced in the next iteration.

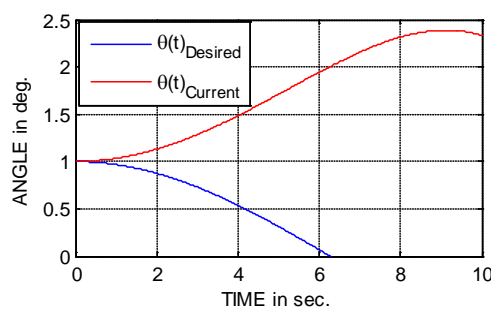


Figure 3.4. The Imitation of the Third Case with Desired and Current Oscillation of the Pendulum.

The optimization algorithm in this step was first chosen to be a golden section search algorithm in order to reduce the need of computational power. However in some cases instead of converging to a solution it diverged from it. Therefore golden section search algorithm is changed with binary search algorithm sacrificing some computational power in order to prevent the algorithm from diverging.

The binary search algorithm starts its search inside a boundary. The lower bound is set to be almost zero. The upper bound is chosen as a very high value which allows the magnetic counterforce to become so powerful that it greatly beats the gravitational force on pendulum; therefore it is ensured that the response of the seismometer is like the third case in Figure 3.4 and the optimum point lies inside the starting boundary. In every iteration the algorithm checks the error function output for the current iteration point, decides to the direction of converging and calculates next iteration point as given in Appendix C.

3.3.2. Oscillation Period Optimization

So far the algorithm in the first step can converge to a magnetic counterforce constant value for a given period. In this step it will be decided how much the desired period value should be increased. The two already known characteristics about the effects of the counterforce constant are that increasing it from zero starts increasing the period and beyond a point it beats up the gravitational force and prevents the pendulum to oscillate. These two characteristics are also tested with the Real Pendulum with Counterforce Model in Simulink. Results are shown in Figure 3.5.

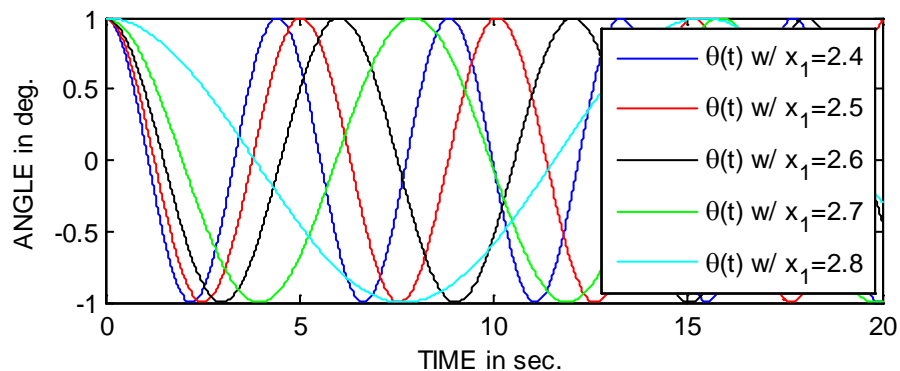


Figure 3.5. Oscillation of the Pendulum with different magnetic counterforce constant values.

These simulations are run with different initial states and different pendulum variables. In all of them the result comes out as confirming the given statement: “As long as the magnetic counterforce constant increases the period increases proportionally and after a blow-up point it hinders a full swing”. So the upper and lower boundary conditions of counterforce constant are known, the conditions in between needs to be simulated and understood.

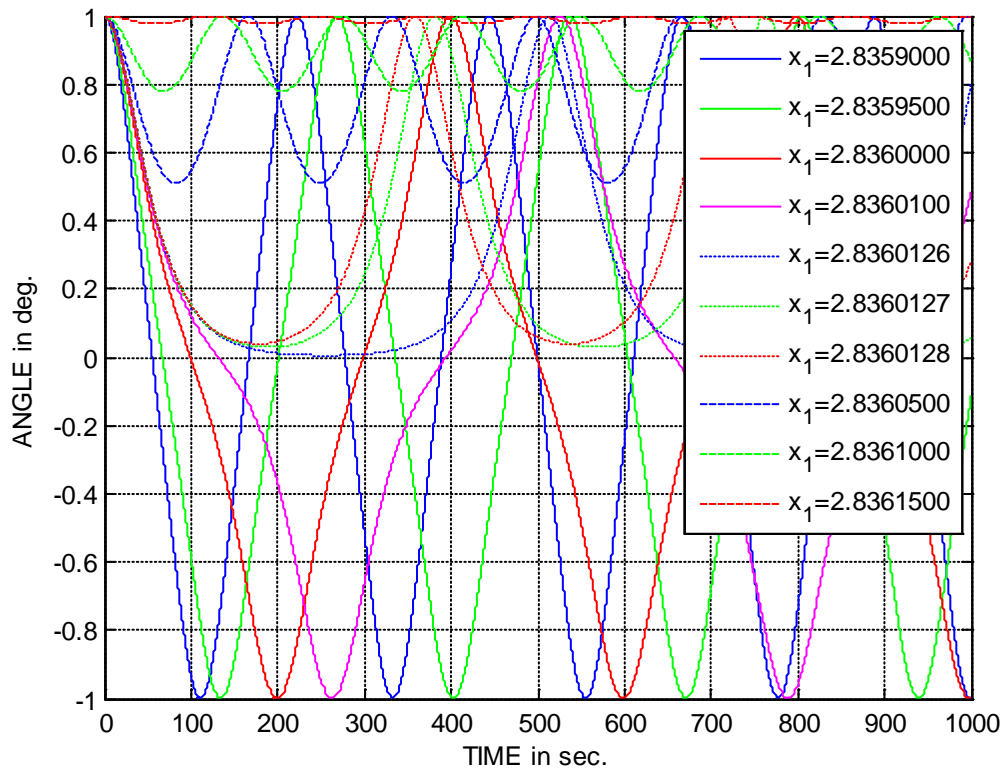


Figure 3.6. Magnetic Counterforce Constant Effect on Pendulum Oscillation.

The simulation results shows that while getting close to the blow-up point the sinusoidal oscillation starts changing its shape as seen in Figure 3.6. This change is unwanted and needs to be avoided. However the oscillation reaches its biggest period value in this area. Therefore the error function supplying the optimization algorithm should be altered in the way that it can detect this shape error too. In every iteration it takes in the dataset, including θ values with respect to time, as an input. Period calculation function written in Matlab calculates the period value of the current oscillation. A real sinusoidal signal with this period value is created by using the simplified pendulum function and

Signal Generator simulink block which are also used in the magnetic counterforce optimization.

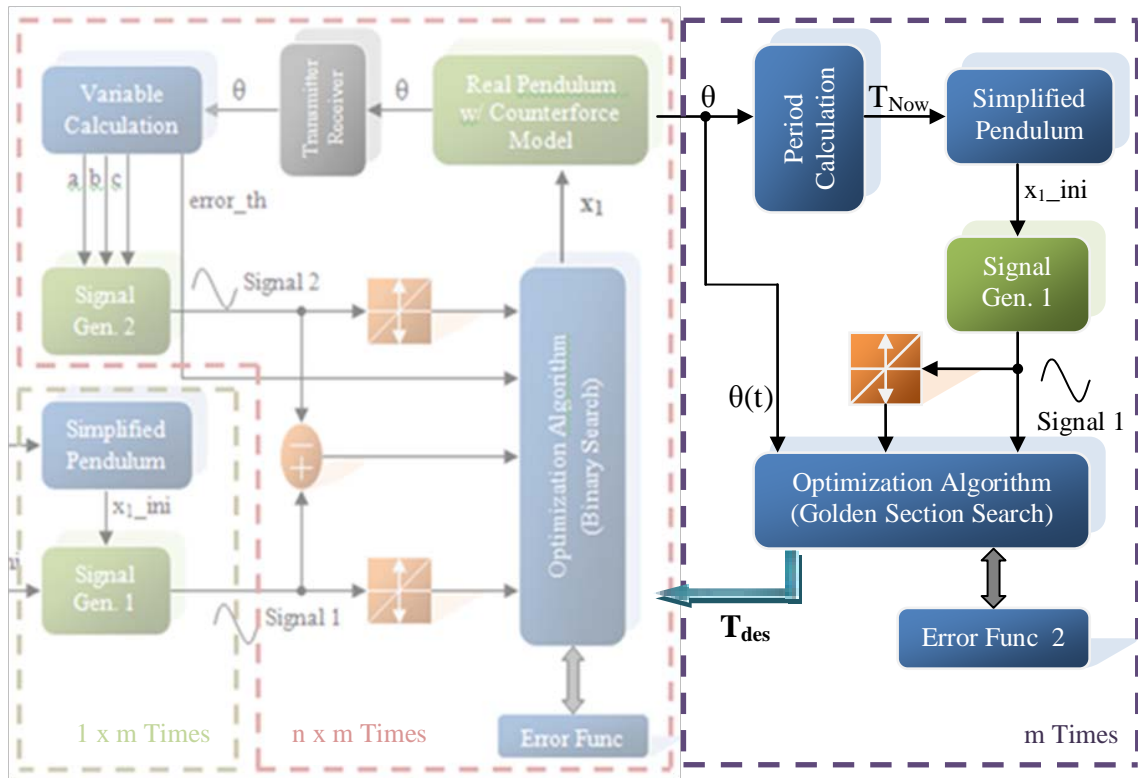


Figure 3.7. Oscillation Period Optimization Diagram (Green Blocks: Models built in Simulink; Blue Blocks: Functions and Algorithms written in Matlab; Black Block: Unnecessary and Discarded Part in Modelling).

One fourth of the period length is not enough for the error function in this step because the shape of the input signal is not known for each case. Therefore at least the half of the period should be checked with the error function. The computational power need for each cycle is not as much important as the previous optimization algorithm because this optimization algorithm calls the previous algorithm n times for its each iteration. Considering this fact it is decided to check the signal for three quarter period length in error function. The optimization algorithm decides on the length of the simulation by checking the zero crossings of the created signal by signal generator block. The simulation starts on the maximum point of the signal one and ends at second zero crossing of it. This algorithm is given in detail in Appendix C. The optimization algorithm improves period value of the desired oscillation in every iteration until the error output is minimized. The algorithm considers the error value as minimized if its change in each iteration goes below

the resolution, namely τ_{gs} . The optimization is based on the golden section search algorithm which is explained in section 3.1.2. The Simulink block “Real Pendulum with Counterforce Model” is run for many different values of counterforce constant. The corresponding period values and error outputs are recorded in a dataset.

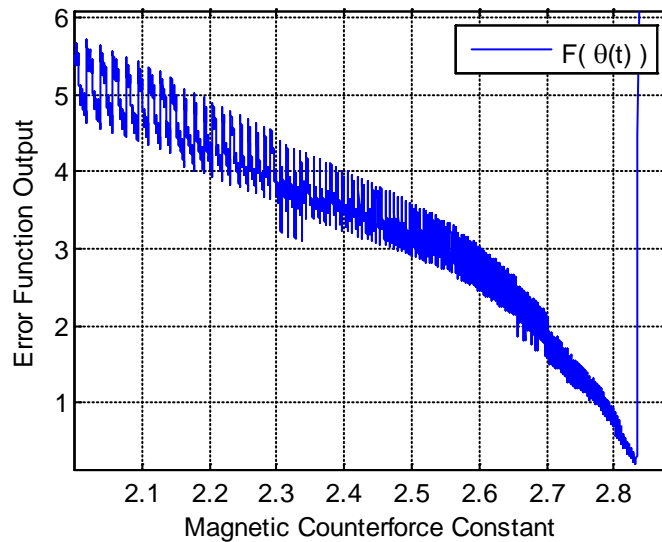


Figure 3.8. Error Output mapped against Magnetic Counterforce Constant.

In Figure 3.8 error output is plotted against its corresponding magnetic counterforce constant value. It is obvious that the error output for increasing counterforce constant values has many local minima and local maxima and also a global minimum. In order to have the Seismometer working at its best condition the magnetic counterforce constant should be arranged such that the error output stays as close as possible to the global minimum.

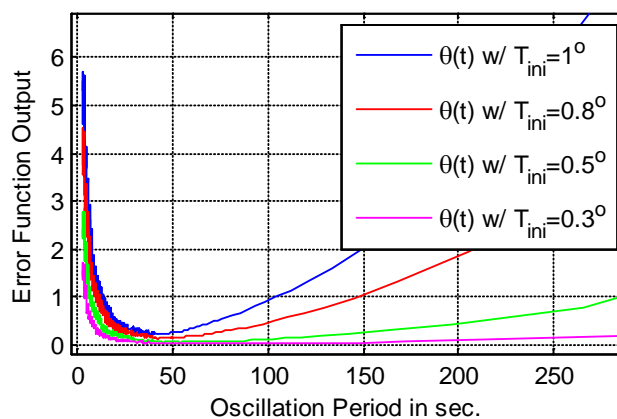


Figure 3.9. Maximum Angle Displacement Effect on Error Output.

The effects of the maximum angle displacement on the pendulum are also tested with different initial angle values. In Figure 3.9 some of them are shown. The error output decreases proportional to the decrease in maximum elongation of the pendulum. This is logical because the simple pendulum behaves like an harmonic oscillator if the maximum elongation goes to zero. As much as this maximum elongation is increased that much the error will increase due to the pendulum dynamics which is calculated in Appendix A.

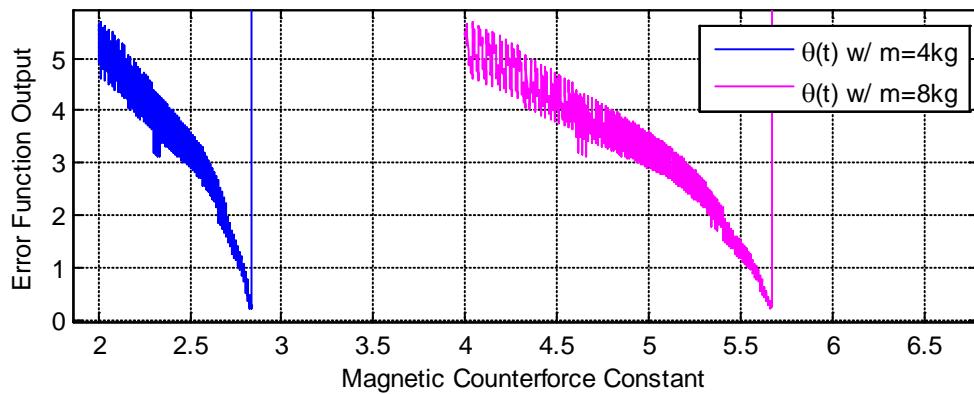


Figure 3.10. The Effect of the Change in Total Pendulum Mass on Error Output.

The mass change effect of the pendulum on the seismometer is also examined. As it can be seen in Figure 3.10 the mass increase doesn't effect the total error output map. However it expands the range of the magnetic counterforce constant where the period is optimized because the total mass increase leads to the need of the total magnetic counterforce increase to cause the same effect on the period of the pendulum. Therefore it makes the optimization easier if it is increased as much as possible in the real world implementation.

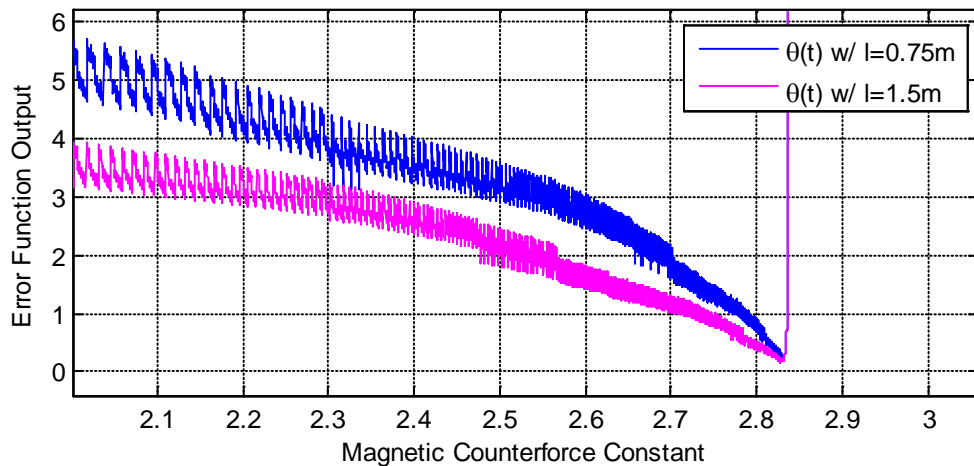


Figure 3.11. The Effect of the Change in Total Pendulum Length on Error Output.

The effect of the change in the total pendulum length on error output is also examined. At the first look on the Figure 3.11 it can be understood that increase in length decreases error output for a given magnetic counterforce constant value. This difference tends to decrease as the magnetic counterforce constant converges to its minimum error point and becomes zero at its minimum point. Therefore it can be assumed that if the pendulum parameters are optimized the length of the pendulum has no effect on the pendulum. However this is not true because length of the pendulum has a small but a non-zero effect on the error output of the pendulum. An increase in the length of the pendulum also implies a smaller maximum angular elongation for the same seismic wave. As it can be seen in Figure 3.9 this fact implies that it will decrease the error output of the pendulum.

4. CONCLUSION

4.1. Summary of Achievements and Conclusion

In this thesis the simulink model of the new SG type Seismometer is built which was found and experimentally built first by the author and M.H.Calayir together in 2004 [7] . The main goal, achieved in this thesis, was to find the problem which hinders the period of the seismometer to be increased over ten seconds. The problem is related with the magnetic counterforce constant value of the seismometer therefore its effects on the pendulum are also studied in detail.

In the first step a fully representative kinematic model of this new seismometer, which uses the magnetic counterforce to have an increased period, is built in matlab (simulink) as seen in Fig 2.13. An increase in the length of the pendulum clearly increases the maximum period value of the seismometer. An increase in the mass of the pendulum doesn't change the maximum period value of the seismometer but it increases the magnetic counterforce constant range which in particular increases the sensitivity of its optimization in real world implementation.

In the second step the effect of changing the magnetic counterforce constant of the seismometer is examined thoroughly. It is found that by increasing the magnetic counterforce constant, the period of the pendulum starts increasing until it reaches the blow up boundary. If the magnetic counterforce constant is increased beyond this value, the pendulum can't complete a full swing. After the mathematical representation of the signal, given in Equation 2.43, is studied, it was seen that by acting a magnetic force on the pendulum its harmonic oscillation is disrupted. However after the simulated test results are examined, it was seen that the magnitude of this error is related to the change of the magnetic counterforce constant. The magnitude of this error shows the particular behavior if it is considered with respect to the change of the counterforce constant: While the magnetic counterforce constant starts to increase beginning from its minimum value, the envelope of the error output shows a stable decrease with an exponentially increasing slope. The amplitude of the ripple becomes also smaller while the magnetic counterforce

constant increases. While converging to the blow up point from left, which totally stops the pendulum to complete its full swings, the error starts to increase with a very high slope. If the blow up point is reached the pendulum can't complete a full swing anymore. This can be seen in Figure 3.8 clearly.

The optimization part of this second step is started with the knowledge gained in the first part. The goal is to design an algorithm which is built such that it can converge to a magnetic counterforce constant value for any given period value, if it is physically possible. This goal is reached by using the binary search method as the optimization algorithm. It requires obtainable computational power and it is stable. This step was planned to be the end of this thesis however it is carried on one step further.

The error, related with the change of the magnetic counterforce constant, has a very sharp minimum point. The second optimization algorithm by using a golden section type search method is built to converge as near as possible to this minimum. This algorithm has given promising results. It converges to the minimum point with every iteration one step further. It doesn't cross to the right hand side of the minimum. This is important because on the right hand side of the minimum the slope of the error function is very high. Therefore a small increase in magnetic counterforce constant causes a rapid increase in the error value. Mapping the whole effect of the change in the magnetic counterforce constant value gives out a better solution than using this optimization algorithm. However this mapping takes 1 to 4 weeks to complete with a good processor unit². The optimization algorithm, which is built with this thesis, requires only 1 to 2 hours to give almost the same results with the same precision.

4.2. Future Work

In this thesis it is proven that the optimization of the magnetic counterforce constant value is the key to increase the period of the new SG type Seismometer. Two methods to find an optimized magnetic counterforce constant value is found and also explained. However a real world implementation method should be developed in order to be able to adjust these parameters in the required resolution. The most basic method is to amplify the signal where the amplification constant is built adjustable with a potentiometer. However if

² Intel Core 2 Quadcore CPU Q6600 @ 2.40 Ghz 4 GB RAM

it covers the whole possible range of the magnetic counterforce constant value, the required precision can't be reached. Now with this algorithm, the minimum error point for magnetic counterforce constant of any SG type seismometer is found as a small range. Therefore a very precise potentiometer can be implemented to the seismometer such that it allows adjusting the magnetic counterforce constant just in this small range with a high precision.

APPENDIX A: PENDULUM PERIOD CORRECTION

An exact analytical solution of the period error of the pendulum oscillation is given as an Jacobian elliptic sinus function [14].

$$\frac{\Delta T}{T_0} = \sum_{n=1}^{\infty} \left(\frac{(2n)!}{2^{2n} (n!)^2} \right)^2 \sin^{2n} \left(\frac{\theta_0}{2} \right) \quad (\text{A.1})$$

$$\begin{aligned} \frac{\Delta T}{T_0} &= \left(\frac{2!}{2^2 \cdot 1!^2} \right)^2 \sin^2 \left(\frac{\theta_0}{2} \right) + \left(\frac{4!}{2^4 \cdot 2!^2} \right)^2 \sin^4 \left(\frac{\theta_0}{2} \right) + \left(\frac{6!}{2^6 \cdot 3!^2} \right)^2 \sin^6 \left(\frac{\theta_0}{2} \right) \\ &+ \left(\frac{8!}{2^8 \cdot 4!^2} \right)^2 \sin^8 \left(\frac{\theta_0}{2} \right) + \left(\frac{10!}{2^{10} \cdot 5!^2} \right)^2 \sin^{10} \left(\frac{\theta_0}{2} \right) + \left(\frac{12!}{2^{12} \cdot 6!^2} \right)^2 \sin^{12} \left(\frac{\theta_0}{2} \right) \\ &+ \dots \end{aligned}$$

$$\sin \theta = \theta - \frac{\theta^3}{3!} + \frac{\theta^5}{5!} - \frac{\theta^7}{7!} + \dots = \sum_{r=1}^{\infty} (-1)^r \frac{\theta^{2r+1}}{(2r+1)!} \quad (\text{A.2})$$

By using Equation A.2, Equation A.3 is found as

$$\begin{aligned} \sin^2 \theta &= \left(\theta - \frac{\theta^3}{3!} + \frac{\theta^5}{5!} - \frac{\theta^7}{7!} + \frac{\theta^9}{9!} - \dots \right)^2 \quad (\text{A.3}) \\ &= \theta^2 - \frac{\theta^4}{3!} + \frac{\theta^6}{5!} - \frac{\theta^8}{7!} + \frac{\theta^{10}}{9!} - \dots \\ &\quad - \frac{\theta^4}{3!} + \frac{\theta^6}{3! \cdot 3!} - \frac{\theta^8}{3! \cdot 5!} + \frac{\theta^{10}}{3! \cdot 7!} - \dots \\ &\quad + \frac{\theta^6}{5!} - \frac{\theta^8}{3! \cdot 5!} + \frac{\theta^{10}}{5! \cdot 5!} - \dots \\ &\quad - \frac{\theta^8}{7!} + \frac{\theta^{10}}{3! \cdot 7!} - \dots \\ &\quad + \frac{\theta^{10}}{9!} - \dots \end{aligned}$$

which implies

$$\begin{aligned}
\sin^4\theta &= (\sin^2\theta)^2 = \theta^4 - 2\frac{\theta^6}{3!} + 2\frac{\theta^8}{5!} + \frac{\theta^8}{3! \cdot 3!} - 2\frac{\theta^{10}}{7!} - 2\frac{\theta^{10}}{3! \cdot 5!} + \dots \\
&\quad - 2\frac{\theta^6}{3!} + 4\frac{\theta^8}{3! \cdot 3!} - 4\frac{\theta^{10}}{3! \cdot 5!} - 2\frac{\theta^{10}}{3! \cdot 3! \cdot 3!} + \dots \\
&\quad + 2\frac{\theta^8}{5!} + \frac{\theta^8}{3! \cdot 3!} - 4\frac{\theta^{10}}{3! \cdot 5!} - 2\frac{\theta^{10}}{3! \cdot 3! \cdot 3!} + \dots
\end{aligned} \tag{A.4}$$

By using Equation A.3 and Equation A.4, Equation A.5 is found as

$$\begin{aligned}
\sin^6\theta &= (\sin^2\theta)(\sin^4\theta) \\
&= \theta^6 - 6\frac{\theta^8}{3!} + 4\frac{\theta^{10}}{5!} + 14\frac{\theta^{10}}{3! \cdot 3!} + 2\frac{\theta^{10}}{5! \cdot 3!} - \dots
\end{aligned} \tag{A.5}$$

Equation A.4 also implies

$$\sin^8\theta = (\sin^4\theta)^2 = \theta^8 - 8\frac{\theta^{10}}{3!} + \dots \tag{A.6}$$

By using Equation A.4 and Equation A.5, Equation A.7 is found as

$$\sin^{10}\theta = (\sin^4\theta)(\sin^6\theta) = \theta^{10} - \dots \tag{A.7}$$

Putting Equation A.3, Equation A.4, Equation A.5, Equation A.6, Equation A.7 into A.1, A.8 is found as

$$\begin{aligned}
\frac{\Delta T}{T_0} &= \left(\frac{2!}{2^2 \cdot 1!^2}\right)^2 \sin^2\left(\frac{\theta_0}{2}\right) + \left(\frac{4!}{2^4 \cdot 2!^2}\right)^2 \sin^4\left(\frac{\theta_0}{2}\right) + \left(\frac{6!}{2^6 \cdot 3!^2}\right)^2 \sin^6\left(\frac{\theta_0}{2}\right) \\
&\quad + \left(\frac{8!}{2^8 \cdot 4!^2}\right)^2 \sin^8\left(\frac{\theta_0}{2}\right) + \left(\frac{10!}{2^{10} \cdot 10!^2}\right)^2 \sin^{10}\left(\frac{\theta_0}{2}\right) + \dots \\
&= \frac{1}{4} \left(\frac{\theta_0^2}{4} - \frac{2\theta_0^4}{16 \cdot 6} + \frac{2\theta_0^6}{64 \cdot 120} + \frac{\theta_0^6}{64 \cdot 6 \cdot 6} - \frac{2\theta_0^8}{256 \cdot 5040} - \frac{2\theta_0^8}{256 \cdot 6 \cdot 120} \right. \\
&\quad \left. + \frac{2\theta_0^{10}}{1024 \cdot 362880} + \frac{2\theta_0^{10}}{1024 \cdot 6 \cdot 5040} + \frac{\theta_0^{10}}{1024 \cdot 120 \cdot 120} - \dots \right) \\
&\quad + \frac{9}{64} \left(\frac{\theta_0^4}{16} - 4\frac{\theta_0^6}{64 \cdot 6} + 4\frac{\theta_0^8}{256 \cdot 120} + 6\frac{\theta_0^8}{256 \cdot 6 \cdot 6} - 2\frac{\theta_0^{10}}{1024 \cdot 5040} \right. \\
&\quad \left. - 10\frac{\theta_0^{10}}{1024 \cdot 6 \cdot 120} - 4\frac{\theta_0^{10}}{1024 \cdot 6 \cdot 6 \cdot 6} + \dots \right)
\end{aligned}$$

$$\begin{aligned}
& + \frac{25}{256} \left(\frac{\theta_0^6}{64} - 6 \frac{\theta_0^8}{256 \cdot 6} + 4 \frac{\theta_0^{10}}{1024 \cdot 120} + 14 \frac{\theta_0^{10}}{1024 \cdot 6 \cdot 6} \right) \\
& \quad \quad \quad + 2 \frac{\theta_0^{10}}{1024 \cdot 120 \cdot 6} - \dots \\
& + \frac{1225}{16384} \left(\frac{\theta_0^8}{256} - 8 \frac{\theta_0^{10}}{1024 \cdot 6} + \dots \right) \\
& + \frac{3969}{65536} \left(\frac{\theta_0^{10}}{1024} - \dots \right) \\
& = \frac{\theta_0^2}{16} - \frac{\theta_0^4}{192} + \frac{9\theta_0^4}{1024} + \frac{\theta_0^6}{5760} - \frac{3\theta_0^6}{2048} + \frac{25\theta_0^6}{16384} - \frac{\theta_0^8}{2580480} - \frac{\theta_0^8}{368640} + \frac{9\theta_0^8}{491520} \\
& + \frac{9\theta_0^8}{98304} - \frac{25\theta_0^8}{65536} + \frac{1225\theta_0^8}{4194304} + \frac{\theta_0^{10}}{743178240} + \frac{\theta_0^{10}}{61931520} + \frac{\theta_0^{10}}{58982400} - \frac{\theta_0^{10}}{18350080} \\
& - \frac{\theta_0^{10}}{524288} - \frac{\theta_0^{10}}{393216} + \frac{5\theta_0^{10}}{1572864} + \frac{175\theta_0^{10}}{4718592} + \frac{5\theta_0^{10}}{18874368} - \frac{1225\theta_0^{10}}{12582912} + \frac{3969\theta_0^{10}}{671108864} \\
& - \dots
\end{aligned}$$

Summing these up gives the error function of pendulum as

$$\begin{aligned}
\frac{\Delta T}{T_0} &= \frac{1}{16} \theta_0^2 + \frac{11}{3072} \theta_0^4 + \frac{173}{737280} \theta_0^6 + \frac{22931}{1321205760} \theta_0^8 \\
& \quad + \frac{1319183}{951268147200} \theta_0^{10} + \dots
\end{aligned} \tag{A.8}$$

and for the maximum elongation of 1° and a period value of 3s the period error comes out as

$$\begin{aligned}
\frac{\Delta T}{3} &= \frac{1}{16} + \frac{11}{3072} + \frac{173}{737280} + \frac{22931}{1321205760} + \frac{1319183}{951268147200} \\
\Delta T &\approx 0.2 \text{ seconds.}
\end{aligned}$$

APPENDIX B: OTHER SEISMOMETER BLOCK FIGURES

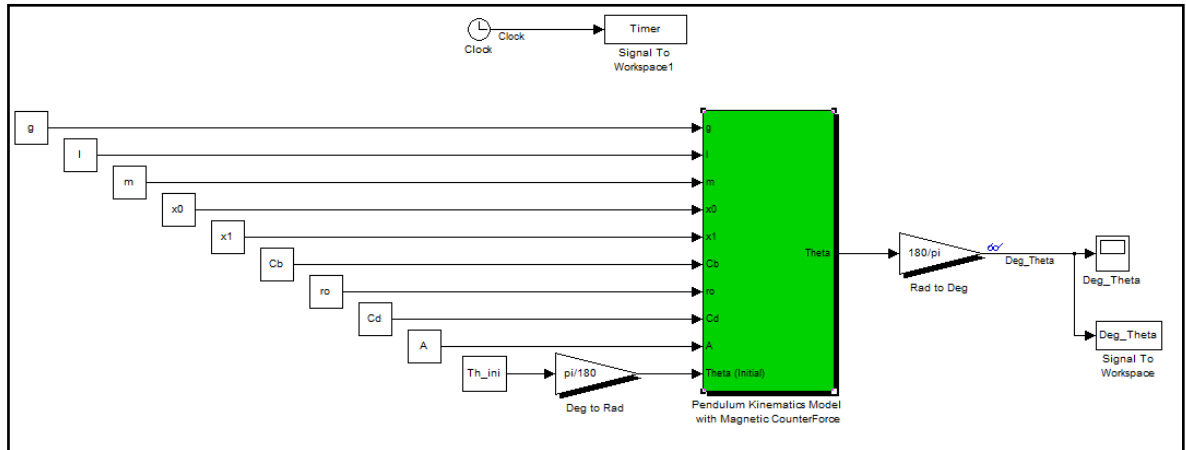


Figure B.1 Real Pendulum Kinematics Model of the new SG Type Seismometer with Magnetic Counterforce (masked).

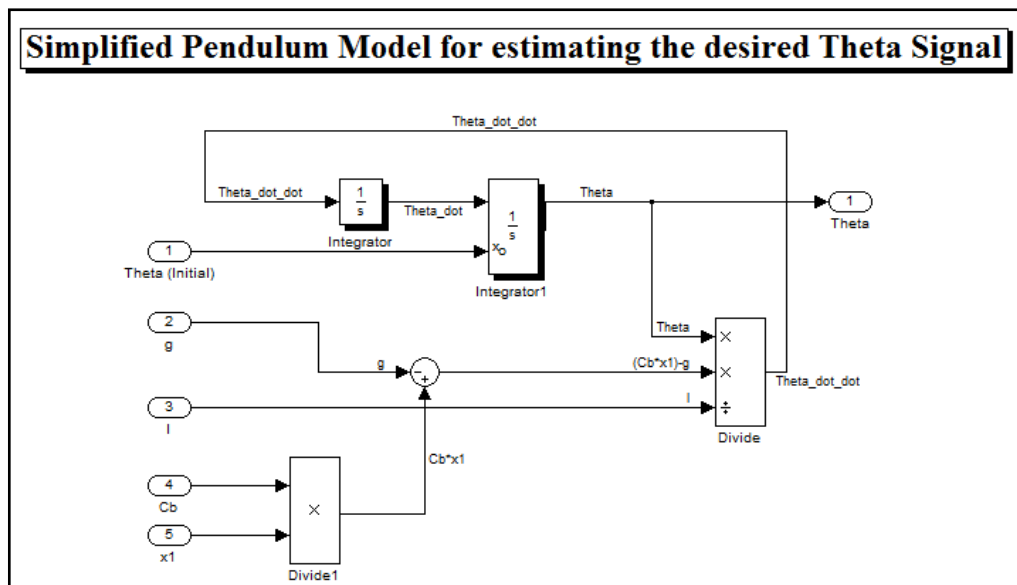


Figure B.2 Simplified Pendulum Model for estimating the desired Theta Signal.

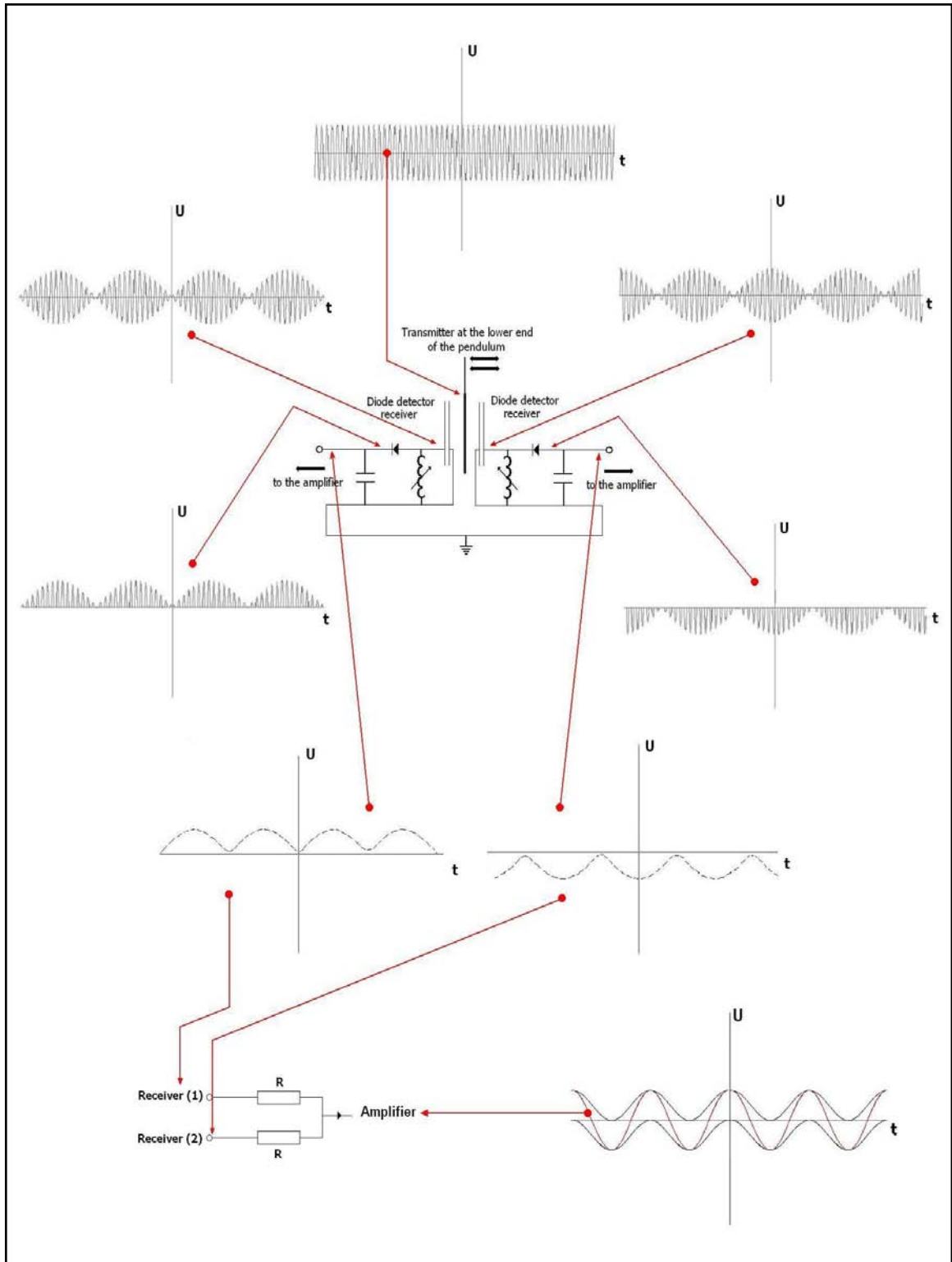


Figure B.3 Transmitter Receiver Part Signal Processing to get the Signal $\theta(t)$ in Real Pendulum [6] .

APPENDIX C: MATLAB ALGORITHMS AND FUNCTIONS

C.1 Error Function of the Magnetic Counterforce Optimization Algorithm

```

function[F_Error]=Func_Error(Hit_Crossing_Sgn_1,Hit_Crossing_Sgn_2,Sgn_1,
Sgn_2,error_Th,Timer)

%Takes in:
%Hit_Crossing_Sgn_1
%Hit_Crossing_Sgn_2
%Timer
%Diff Signal (Sgn_3=Sgn_1-Sgn_2)
%error_Th

%Gives out:
%Error Function Value (F_Error)

Sgn_3=zeros(max(size (Sgn_1,1),size (Sgn_2,1)),1); % Creating the Diff
Signal (Sgn_3=Sgn_1-Sgn_2) without data
i_err=1; %counter for Diff Signal (dummy_deneme = -3;)

if(error_Th==1) % If the pendulum goes over the edge and does not
swing back and forward then this error_Th (Theta error occurs)
    F_Error=-123456789; % So we initialize the error output to a maximum
in this case
elseif(error_Th==0) % If this is not the case, we calculate the error
below

    while (i_err <= (min(size (Sgn_1,1),size (Sgn_2,1)))) % Loading all
the diff. data to Sgn_3
        Sgn_3(i_err,1)=Sgn_1(i_err,1)-Sgn_2(i_err,1); % until one
of the signals hits zero
        if(Hit_Crossing_Sgn_1(i_err,1)== 1) % We check at
each step whether one of
            break % the signals
Hits the Zero

```

```

elseif (Hit_Crossing_Sgn_2(i_err,1)== 1)           % If this is
the case so we terminate
break                                             % the
process.
end
i_err=i_err+1;
end

i_err_2=1;
F_Error=0;
while (i_err_2 <= i_err)                         % Summing up the
error at this variable for later check
F_Error=F_Error+Sgn_3(i_err_2,1);               % in the optimisation
code. This will be the error output
i_err_2=i_err_2+1;                               % of the function.

end
F_Error=F_Error/Timer(i_err,1);                  % Dividing the error
sum to the passed time
% which is needed
because of the changing process
% time at each Error
check (Because Zero hitting time
% of Signals will
% change at each
optimisation step)

end
%%%%----- END -----%%%%%%%%

```

C.2 Variable Calculation Algorithm

```

function[a,b,c,error_Th]=Func_Var(Deg_Theta,Timer,Th_ini)
%%% Matlab Function to calculate a , b & c & error_Th %%%
%%% Th_ini*cos(b*t+c)=Deg_Theta
%%%-----%%%%%%%%
i=2;
error_Th=0;
i_max=size(Deg_Theta,1);

```

```

while(i<=i_max && Deg_Theta(i,1)>0 ) %Getting Zero crossing time for
Signal Deg_Theta
    if(Deg_Theta(i-1,1)<Deg_Theta(i,1)) %Check whether function is
getting larger or smaller (Model Blow-up Control)
        error_Th=1; %Give error if counter force is growing larger than
the gravitational force.
            a=1;
            b=1;
            c=0;
            break;
        end;
        i=i+1;
    end
t_dummy=Timer(i-1,1); %recording time initial.

if(error_Th==0)
    a=Th_ini; %Amplitude is equal to the initial theta value.
    c=acos((Deg_Theta(1,1)/Th_ini)); %This should come out zero (Because
it is the Phase
    b=(acos(0)-c)/t_dummy; %Frequency should be calculated,
end

```

C.3 Period Calculation Algorithm

```

function [T_Out]=Calc_T_Signal(Signal,Timer,Period)
%   Function Should Take inside:
%   1) Data set of the signal values
%   2) and its own Timer output values set
%   3) Number of Periods over which we should look to calculate T.
%
%   And it gives out Period Time T
%
%   ASSUMPTION "Signal Should Start with a Positive Elongation!" In our
%   case this assumption is fulfilled.
%
N_ZC=(Period*2)+1;           % Number of ZeroCrossings needed to pass
                             % until the desired number of Periods
reached.

i=0;

```

```

j=1;
j_max=size(Signal,1);
while(Signal(j,1)>=0 && j<j_max)      % Signal reaches zero with
negative derivative first time.
    j=j+1;
end
T_Start=Timer(j,1);      % Store the timer output of this step.(As
starting point)
i=i+1;
while (i<N_ZC)
    while(Signal(j,1)<=0 && j<j_max)    % Signal reaches zero with
positive derivative .
        j=j+1;
    end
    i=i+1;
    while(Signal(j,1)>=0 && j<j_max)    % Signal reaches zero with
negative derivative .
        j=j+1;
    end
    i=i+1;
end
T_End=Timer(j,1);      % Store the timer output of this step.(As
end point)

if(T_End==T_Start)      % j eger j_max sevitesine ulaşırsa yani
Periyodunu ölçmek istediğimiz sinyal hiç sifıra ulaşmıyorsa Periyodu
maximum olarak geriye döndür.
    T_Start=0;
end
T_Out=(T_End-T_Start)/Period;

```

C.4 Optimization Algorithms calling Simulink blocks and other Functions to converge to the desired period and magnetic counterforce constant value

```

gs_cnt=1;      %%%%%%%%%Golden Section Count for Total End Error and
Tdes optimisation%%%%%%%%
phi=(1+5^0.5)/2;      % Golden Ratio (phi)= 1.6180
tau_gs=1;      % Tau (Sensitivity of Goldensection Pendulum Search)
Gs_Output_Array=zeros(50,8);

```

```

T_a=0;
T_b=0;
T_c=0;
T_d=0;
FT_a=0;
FT_b=0;
FT_c=0;
FT_d=0;

while(gs_cnt<50)
    if(gs_cnt==1)
        Tdes=Tdes;
        T_a=Tdes;          % Search Range starts from Tdes
    elseif(gs_cnt==2)
        Tdes=Tend;
        T_b=Tend;        % Search Range goes up to Tend %%%---Boundry
        Condition---%%
    elseif(gs_cnt==3)

        % Calculation of first golden section of the range
        % a = d_a Distance a (which is T_c-T_a)
        % b = d_b Distance b (which is T_b-T_c)
        %   T_b-T_a = a+b
        %   T_b-T_a = a+(phi*a)
        %   T_b-T_a = a(1+phi)
        %           a =(T_b-T_a)/(1+phi)
        d_a=(T_b-T_a)/(1+phi);
        T_c=T_a+d_a;      % Adding diff. between T_a and T_c gives
us
                           % the first golden section of the boundry
        (T_c)
        Tdes=T_c;
    else
        %%%---- Calculating new golden section ----%%
        if(T_b-T_c>T_c-T_a)          %CASE 1
            T_d=T_a+(T_b-T_c);
        else                          %CASE 2
            T_d=T_b-(T_c-T_a);
        end
        Tdes=T_d;

```

```

        if(abs(T_b-T_a)<tau_gs)          % Checking whether the search area
is narrowed enough in Goldensection Search.
            T_Gs =(T_a+T_b)/2
            break
        end
    end
end

%%%----- Calculating X1 Initial -----%%%%%%%%%
x1_ini=((g-((1*4*pi^2)/Tdes^2))/Cb); %Calculated from the formula
Serwey 6E (P:457 Formula 15.13)
%%%-----.....-----%%%%%%%%%

x1=x1_ini;
%%%-----Running Reference Pendulum Model-----%%%%%%%%%
sim('Cosine_Gen_1.mdl',Tdes)
%%%-----.....-----%%%%%%%%%

%%%%%%%%----- OPTIMISATION OF X1 TO REACH Tdes VALUE -----%%%%%%%%

phi=(1+5^0.5)/2;          % No need to Golden Ratio (phi)= 1.6180
Because of

                                % using BINARY SEARCH in this optimization
tau=0.0001;                    % Tau (Sensitivity of Goldensection Pendulum
Search)
x1_a=x1_ini;                    % Search Range starts from x1_a
x1_b=1000;                      % Search Range goes up to x1_b=1000 %%%---
Boundry Condition---%%%
s_w=0;                          % Binary Search Error check (Something Wrong)

%%%----- GETTING ERROR FUNCTION OUTPUT FOR x1_a -----%%%%%%%%%

%%%%%%%% --- INITIALISATION --- %%%%%%%%%
x1=x1_a;
%%%-----Running Real Pendulum Model-----%%%%%%%%%
sim('Pendulum_Model_5_BForce_Subsystemed.mdl',Tdes);
%%% Matlab Function to calculate a , b & c & error_Th %%%
[a,b,c,error_Th]=Func_Var(Deg_Theta,Timer,Th_ini);

```



```

    %%----- Cosine Generator__Signal_2 (Simulating pendulum current
oscillation)---%%
    sim('Cosine_Gen_2.mdl',Tdes);
    %%%-----RUNNING ERROR FUNCTION OF THE SG-PENDULUM MODEL ----%%

fx1_a=Func_Error(Hit_Crossing_Sgn_1,Hit_Crossing_Sgn_2,Sgn_1,Sgn_2,error_
Th,Timer);
    %%%-----.....-----%%

    %%----- GETTING ERROR FUNCTION OUTPUT FOR x1_b -----%%
x1=x1_b;
    %%-----Running Real Pendulum Model-----%%
sim('Pendulum_Model_5_BForce_Subsystemed.mdl',Tdes);
    %% Matlab Function to calculate a , b & c & error_Th %%
[a,b,c,error_Th]=Func_Var(Deg_Theta,Timer,Th_ini);
    %%----- Cosine Generator__Signal_2 (Simulating pendulum current
oscillation)---%%
    sim('Cosine_Gen_2.mdl',Tdes);
    %%%-----RUNNING ERROR FUNCTION OF THE SG-PENDULUM MODEL ----%%

fx1_b=Func_Error(Hit_Crossing_Sgn_1,Hit_Crossing_Sgn_2,Sgn_1,Sgn_2,error_
Th,Timer);
    %%%-----.....-----%%

    i_bs_count=1;
    while (i_bs_count<201)           % Binary Search algorithm limited to
200 Loops.
        i_bs_count=i_bs_count+1;

        if(abs(x1_b-x1_a)<tau)       % Checking whether the search area is
narrowed enough.
            x1=(x1_a+x1_b)/2
            break
        else

            %Binary Type Search Optimized for calculating Backforce
constant
            %using Pendulum Model Blocks with Backforce manipulation and
created Matlab
            %Functions for estimating SG-Seismograph Period length.

```

```

%%%---- Calculating new binary section ----%%%
x1_c=(x1_a+x1_b)/2;
%%%-----.....-----%%%%%%%%

%%----- GETTING ERROR FUNCTION OUTPUT FOR x1_c -----%%%%%%%%
x1=x1_c;
%%-----Running Real Pendulum Model-----%%%%%%%%
sim('Pendulum_Model_5_BForce_Subsystemed.mdl',Tdes);
%% Matlab Function to calculate a , b & c & error_Th %%
[a,b,c,error_Th]=Func_Var(Deg_Theta,Timer,Th_ini);
%%----- Cosine Generator__Signal_2 (Simulating pendulum
current oscillation)---%%
sim('Cosine_Gen_2.mdl',Tdes);
%%%%%%%%-----RUNNING ERROR FUNCTION OF THE SG-PENDULUM MODEL --
--%%%%%%%%

fx1_c=Func_Error(Hit_Crossing_Sgn_1,Hit_Crossing_Sgn_2,Sgn_1,Sgn_2,error_
Th,Timer);

%%%%%%%%-----.....-----%%%%%%%%

if(fx1_c>0)                %CASE 1
    if(fx1_c <= fx1_a)
        x1_a=x1_c;
        fx1_a=fx1_c;
    else
        s_w=1;
    end

elseif(fx1_c<0)           %CASE 2
    if(fx1_c >= fx1_b)
        x1_b=x1_c;
        fx1_b=fx1_c;
    else
        s_w=1;
    end
else
    s_w=0.5;
end
end

```

```

end

%%%--- Here alg. has converged to a new Period T ---%%%
% Lets measure it.
% To measure this we run our real Pendulum Model long enough to take
5
% period long measurement
sim('Pendulum_Model_5_BForce_Subsystemed.mdl',1000);
x1_store=x1;

% Calculating the Period length of the real pendulum
T_Now=Calc_T_Signal(Deg_Theta,Timer,1);

% Calculating the needed x1 for creating the simulated Pendulum Theta
output with Period T_Now
x1_ini=((g-((1*4*pi^2)/T_Now^2))/Cb); %MODEL "Cosine_Gen_1.mdl"
uses x1_ini for Backforce constant%

% Simulating Reference Pendulum Model
sim('Cosine_Gen_1.mdl',1000)

%%%%%%%%----- Calculate the additive error of the function over a 3/4
period ----%%%%%%%%

Sgn_Error=zeros(max(size (Deg_Theta,1),size (Sgn_1,1)),1); %
Creating the Diff Signal without data
i_er=1; %counter for Diff Signal (dummy_deneme = -3;)
count_cross=0;

while (i_er <= (min(size (Deg_Theta,1),size (Sgn_1,1)))) % Loading
all the diff. data to Sgn_Error
Sgn_Error(i_er,1)=Sgn_1(i_er,1)-Deg_Theta(i_er,1); % until
one of the signals hits zero
if(Hit_Crossing_Sgn_1(i_er,1)== 1) % We check
at each step whether Sig_1 crosses Zero
count_cross=count_cross+1;
end

if (count_cross == 2) % If it crosses Zero twice, we
terminate the process nowing that the time passed is equal to 3/4*T

```

```

        break
    end
    i_er=i_er+1;
end

i_er_2=1;
F_Error_Gs=0;
while (i_er_2 <= i_er) % Summing up
the error at this variable for later check
    F_Error_Gs=F_Error_Gs+abs(Sgn_Error(i_er_2,1)); % in the
optimisation code. This will be the error output
    i_er_2=i_er_2+1; % of the
function.
end
F_Error_Gs=F_Error_Gs/Timer(i_er,1) % Dividing
the error sum to the passed time

% which is needed because of the changing process
% time at each Error check (Because Zero hitting time
% of Signal 1 will
% change at each optimisation step)

x1=x1_store; % Write calculated & stored x1 at
lines 42&94
% Which is achieved x1 value for real pendulum model

%%%--- Golden Section Optimisation Output Calculations ---%%%

if(gs_cnt==1)
    FT_a=F_Error_Gs; % Error Output of Starting condition T_a

elseif(gs_cnt==2)
    FT_b=F_Error_Gs; % Error Output of Bonudry condition T_b

elseif(gs_cnt==3)
    FT_c=F_Error_Gs; % Error Output of First Golden Seciton T_c

else

```

```

FT_d=F_Error_Gs;          % Error Output of New Golden Section T_d

if(T_d-T_c>0)             %CASE 1  New Golden Section is
choosen(T_d) on the right hand side
    if(FT_d >= FT_c)
        T_b=T_d;
        FT_b=FT_d;
    else
        T_a=T_c;
        T_c=T_d;
        FT_a=FT_c;
        FT_c=FT_d;
    end

else                       %CASE 2  New Golden Section is
choosen(T_d) on the left hand side
    if(FT_d > FT_c)
        T_a=T_d;
        FT_a=FT_d;
    else
        T_b=T_c;
        T_c=T_d;
        FT_b=FT_c;
        FT_c=FT_d;
    end
end

end

Gs_Output_Array(gs_cnt,:)=[T_a,T_b,T_c,T_d,FT_a,FT_b,FT_c,FT_d];

gs_cnt=gs_cnt+1          % Golden Section Optimisation counter
increase.

end

```

```

        gs_cnt=gs_cnt+1           % Golden Section Optimisation counter
increase.

end

```

C.5 An Example of the Long Term Data Collection Algorithms

```

row=1;
%xl=4;
m=16;
xl=2.8+(row/100000);
Data_Collected_mass_16=ones(100002,5);
while (xl<3.00000)

    %%%--- Here alg. has converged to a new Period T ---%%%
    % Lets measure it.
    % To measure this we run our real Pendulum Model long enough to take
5
    % period long measurement
    xl_store=xl;
    sim('Pendulum_Model_5_BForce_Subsystemed.mdl',1000);

    % Calculating the Period length of the real pendulum
    T_Now=Calc_T_Signal(Deg_Theta,Timer,1);

    %Calculating the needed xl for creating the simulated Pendulum Theta
output with Period T_Now
    xl_ini=((g-((1*4*pi^2)/T_Now^2))/Cb);    %MODEL "Cosine_Gen_1.mdl"
uses xl_ini for Backforce constant%

    % Simulating Reference Pendulum Model
    sim('Cosine_Gen_1.mdl',1000)

    %Calculate the additive error of the function over a 3/4 period

    Sgn_Error=zeros(max(size (Deg_Theta,1),size (Sgn_1,1)),1); %
Creating the Diff Signal without data
    i_er=1;           %counter for Diff Signal (dummy_deneme = -3;)
    count_cross=0;

```

```

        while (i_er <= (min(size (Deg_Theta,1),size (Sgn_1,1)))) % Loading
all the diff. data to Sgn_Error
            Sgn_Error(i_er,1)=Sgn_1(i_er,1)-Deg_Theta(i_er,1); % until
one of the signals hits zero
            if(Hit_Crossing_Sgn_1(i_er,1)== 1) % We check
at each step whether Sig_1 crosses Zero
                count_cross=count_cross+1;
            end

if (count_cross == 2) % If it crosses Zero twice, we terminate
the process.
    break
end
    i_er=i_er+1;
end

    i_er_2=1;
    F_Error_Out=0;
    while (i_er_2 <= i_er) % Summing up
the error at this variable for later check
        F_Error_Out=F_Error_Out+abs(Sgn_Error(i_er_2,1)); % in the
optimisation code. This will be the error output
        i_er_2=i_er_2+1; % of the
function.
    end
    F_Error_Out=F_Error_Out/Timer(i_er,1); % Dividing
the error sum to the passed time

    % which is needed because of the changing process
    % time at each Error check (Because Zero hitting time
    % of Signal 1 will
    % change at each optimisation step)

    %x1=x1_store; % Write calculated & stored x1 at
lines 42&94
    % Which is achieved x1 value for real pendulum model

    Data_Collected_mass_16(row,:)= [row,x1,x1_store,T_Now,F_Error_Out];

    x1=x1+0.00001;

```

```
        row=row+1;  
end  
m=4;
```


REFERENCES

1. Ammon, C. J., *Seismic Waves and Earth's Interior*, 2011, http://eqseis.geosc.psu.edu/~cammon/HTML/Classes/IntroQuakes/Notes/waves_and_interior.html, accessed at December 2011.
2. Nedham, J., *Science and Civilization in China, Volume 3: Mathematics and the Sciences of the Heavens and the Earth*, Cambridge University Press, Cambridge, 1959.
3. Sparks, R., *The C Spring Seismometer*, 2005, <http://www.fairpoint.net/~sparksite/CSpring%20Seismometer.html>, accessed at January 2012.
4. Güralp Systems, *Ocean Bottom Systems*, 2012, <http://www.guralp.com/product-range/ocean-bottom-systems>, accessed at February 2012.
5. Walker, J., *How to build a simple seismograph to record earthquake waves at home*, 2010, <http://psn.quake.net/lehmntxt.html>, accessed at February 2012.
6. Shackelford, B., J. Gundersen, "The Amateur Scientist: Electronic stratagems are the key to making a sensitive seismometer", *Scientific American*, pp. 182-187, 1975.
7. Cakan, M., M. H. Calayir, *Seismograph Based on Proportional Elongations with an Electromagnetically Increased Period*, Participation Report on 16. EU Contest for Young Scientists, Bogazici University, 2004.
8. Calayir, M. H., G. Kaki, B. Mustecapoglu, *Seismometer Based on Displacement proportionality with increased Period*, B.Sc. Thesis, Bogazici University, 2010.
9. Batchelor, G.K., *An Introduction to Fluid Dynamics*, Cambridge University Press, New York, 2000.
10. Serway, R. A., J.W. Jewett, *Physics for Scientists and Engineers*, Eighth Edition, Mary Finch, Belmont, 2009.
11. Boyd, S., L. Vandenberghe, *Convex Optimization*, Cambridge University Press, New York, 2004
12. Bertsekas, D. P., *Nonlinear Programming*, 13th edition, University of Chicago Press, Chicago, 1982.

13. Press, W. H., S. A. Teukolsky, W. T. Vetterling, B. P. Flannery, *Numerical Recipes The Art of Scientific Computing*, Third Edition, Cambridge University Press, New York, 2007.
14. Nelson, R. A., M. G. Olsson, *The Pendulum-Rich Physics from a Simple System*, Research Paper, University of Maryland, 1985 .